Robust increase of Indian monsoon rainfall and its variability under future warming in CMIP-6 models

Anja Katzenberger[1,2], Jacob Schewe[1], Julia Pongratz[2,3], and Anders Levermann[*1,4,5]

[1]Potsdam Institute for Climate Impact Research, Potsdam, Germany
[2]Ludwig-Maximilian University, Munich, Germany
[3]Max Planck Institute for Meteorology, Hamburg, Germany
[4]LDEO, Columbia University, New York, USA
[5]Potsdam University, Potsdam, Germany

Correspondence: [*]Anders Levermann (anders.levermann@pik-potsdam.de)

Abstract. The Indian summer monsoon is an integral part of the global climate system. As its seasonal rainfall plays a crucial role in India's agriculture and shapes many other aspects of life, it affects the livelihood of a fifth of the world's population. It is therefore highly relevant to assess its change under potential future climate change. Global climate models within the Coupled Model Intercomparison Project Phase 5 (CMIP-5) indicated a consistent increase in monsoon rainfall and its variability under global warming. Since the range of the results of CMIP-5 was still large and the confidence in the models was limited due to partly poor representation of observed rainfall, the updates within the latest generation of climate models in CMIP-6 are of interest. Here, we analyse 32 models of the latest CMIP-6 exercise with regard to their annual mean monsoon rainfall and its variability. All of these models show a substantial increase in June-to-September (JJAS) mean rainfall under unabated climate change (SSP5-8.5) and most do also for the other three Shared Socioeconomic Pathways analyzed (SSP1-2.6, SSP2-4.5, SSP3-7.0). Moreover, the simulation ensemble indicates a linear dependence of rainfall on global mean temperature with high agreement between the models and independent of the SSP if global warming is the dominant forcing of the monsoon dynamics as it is in the 21st century; the multi-model mean for JJAS projects an increase of 0.33 mm/day and 5.3% per degree of global warming. This is significantly higher than in the CMIP-5 projections. Most models project that the increase will contribute to the precipitation especially in the Himalaya region and to the northeast of the Bay of Bengal, as well as the west coast of India. Interannual variability is found to be increasing in the higher-warming scenarios by almost all models. The CMIP-6 simulations largely confirm the findings from CMIP-5 models, but show an increased robustness across models with reduced uncertainties and updated magnitudes towards a stronger increase in monsoon rainfall.

1 Introduction

As one of the integral components of the global climate system, the Indian monsoon provides water to the densely populated region of South Asia. About 80% of the annual precipitation over India occurs during the summer period supplying water to the crops during the prime agricultural season (Bollasina, 2014). The crop yields (especially rice is dominant in the region) are highly sensitive to the monsoon rainfall variability (Prasanna, 2014; DeFries et al., 2016). As agriculture contributes to

about 20% of the gross domestic product (Zaveri et al., 2016), the monsoon's rainfall also has an effect on India's economy (Gadgil and Gadgil, 2006). Therefore, there is an inextricable link between the Indian summer monsoon and the health as

25 well as the socio-economic well-being of people. Thus, understanding the response of the Indian summer monsoon and its interannual variability to different global warming scenarios is critical for designing management strategies of water resources and agricultural policies in the future.

In order to understand future projections about potential changes in the monsoon rainfall, it is crucial to understand historic changes and their underlying forcings. In this context, it is important to distinguish between external and internal drivers. Ex-

30 ternal drivers can be of natural (insolation changes due to changes in orbital parameters, volcanic aerosols) and anthropogenic (greenhouse gases - GHG, aerosols, land use change) origin, whereas internal drivers refer to variations based on the interaction within the climate system (air, sea, sea ice, land) (Seth et al., 2019). While orbital forcing mainly shaped the changes of monsoon rainfall on multi-millennial paleoclimatic timescales, anthropogenic forcings competed during the 20th century and since the early 21st century, GHG is dominating as an external forcing (Wang et al., 2005a; Ming et al., 2020; Seth et al., 2019).

35 Multi-millennial paleorecords indicate strong changes both in the Indian and East Asian summer monsoon. These paleoclimatic changes have been revealed by e.g. oxygen isotope analysis from different caves in Asia for the past thousands of years (Wang et al., 2008; Zhang et al., 2008, 2019; Wang et al., 2005b), by analyzing marine sediment records for the Neogene and Quaternary (Wang et al., 2005a), and other methods (Li et al., 2017; Wang et al., 2017; Ming et al., 2020; Wang et al., 2020). Most studies link the paleoclimatic changes of monsoon rainfall predominantly to solar insolation variations on the northern

40 hemisphere affecting the Intertropical Convergence Zone (ITCZ) position due to orbital forcing changes (Wang et al., 2005a, b, 2008; Zhang et al., 2008, 2019; Ming et al., 2020).

Especially to explain abrupt non-linear monsoon transitions as observed in the Holocene in the Tibetan Plateau, gradual insolation changes are not sufficient and thus, internal feedback mechanisms seem to be at play (Schewe et al., 2012; Herzschuh et al., 2014; Boos and Korty, 2016; Wang et al., 2020). The moisture-advection feedback (Levermann et al., 2009) might be

45 such an internal mechanism that is able to provoke abrupt transitions and might be responsible for the abrupt Tibetan Plateau transitions in the Holocene (Herzschuh et al., 2014). Other amplifying effects might have occurred due to a water vapour and cloud feedback (Jalihal et al., 2019).

Observations of the Indian summer monsoon in central India have revealed a decreasing rainfall trend in the second half of the 20th century (Ramanathan et al., 2005; Bollasina et al., 2011; Mishra et al., 2012, 2014b; Shah and Mishra, 2016; Jin and

50 Wang, 2017). Since orbital forcing is playing a negligible role in external forcing in the current centuries (Seth et al., 2019), the competing effects of external anthropogenic forcings are dominating these long-term trends: Anthropogenic forcings are first the effect of GHG and second, the effect of sulfate aerosols and land-surface changes (Singh et al., 2019). The weakening trend of the Indian monsoon is associated with the GHG induced warming of the Indian Ocean sea surface and the fact that the concurrent warming over the Indian subcontinent was dampened due to aerosols and land-cover changes (Zhou et al., 2008;

55 Deser et al., 2010; Seth et al., 2019). The dampening effect over land results from the steep rise of anthropogenic emissions including sulfate aerosols in India and neighboring regions as well as enormous changes in the land cover since the 1950s due to the strong expansion of industry and the population growth (Acharya and Sreekesh, 2013; Krishna Moorthy et al., 2013).

The Indian ocean warming has been linked to anomalies in the lower and upper troposphere due to enhanced latent heat uplift resulting from convection over the ocean (Danielsen, 1993; Dai et al., 2013). The warming of the Indian ocean could intensify the convection over the ocean which is compensated by the subsidence of air masses over land. By preventing the convection over the subcontinent, the Hadley cell is modulated in such a way that a drying trend over the region is introduced (Roxy et al., 2015). Another significant aspect contributing to the rainfall decrease is discussed to be the narrowing of the ITCZ and correspondingly, the decrease of the associated belt of intense rainfall (Byrne and Schneider, 2016).

The declining trend has reversed in various datasets since the beginning of the 21st century, except in the Indian Meteorological Department dataset where a stabilization was captured (Jin and Wang, 2017). The revival of the rainfall in central and north India might be explained by the emerging land warming due to GHG emissions dominating over the effect of sulfate aerosols and land-cover change. The compensating effect of aerosols in particular has declined and is expected to further decline due to policy interventions (Seth et al., 2019; Allan et al., 2020). The decreased ocean evaporation in the Arabian Sea leads to a decrease of moisture transport to India and thus fewer low clouds which results in a warming of the Indian subcontinent. The rising land surface temperature increases the meridional temperature gradient in the lower troposphere, enhancing the Hadley circulation and summer monsoon rainfall (Jin and Wang, 2017). Therefore, the magnitude of future monsoon rainfall may depend on where temperature rises faster – on the sea surface or land masses (Singh et al., 2019). Since this goes back to the competing influence of GHG and aerosol forcing over land, the task of modeling the future monsoon rainfall coincides with projecting the magnitude of the different forcing mechanisms and capturing the monsoon's sensitivity to it.

Within the latest studies using global coupled models, there is a widespread consensus that the Indian monsoon rainfall will increase due to climate change in the 21st century (Chaturvedi et al., 2012; Menon et al., 2013; Lee and Wang, 2014; Asharaf and Ahrens, 2015; Mei et al., 2015; Sharmila et al., 2015; Varghese et al., 2020). This trend is found for various CMIP-5 models (Menon et al., 2013), the multi-model mean (Chaturvedi et al., 2012), the mean of only the four best models (Lee and Wang, 2014) or the model with the best deep convection scheme (Varghese et al., 2020). Under Representative Concentration Pathway 8.5 (RCP-8.5) CMIP-5 models project a median increase in Indian monsoons rainfall of 2.3%/K (Menon et al., 2013). Also under RCP-8.5, the amount of rainfall over India is projected to increase by 18.7% by the end of the 21st century compared to 1961-1999 (Chaturvedi et al., 2012). This trend is expected to be the consequence of the warming of the Indian Ocean enhancing atmospheric moisture content and thus moisture flux convergence arising from changes in moisture which generally follow the Clausius-Clapeyron relation (Cherchi et al., 2011; Seth et al., 2013; Mei et al., 2015; Sooraj et al., 2015; D'Agostino et al., 2019). This so called thermodynamic effect dominates over the dynamic effect which refers to weaker winds and a reduced monsoon circulation due to a weakened tropical overturning circulation and an expected decrease of rainfall (Vecchi et al., 2006; Mei et al., 2015; Sooraj et al., 2015; D'Agostino et al., 2019). Besides, the interannual variability is projected to increase in most models under the strongly forced scenarios as well as in models with good performance in capturing the mean seasonal cycle in the present climate (Kitoh et al., 1997; Menon et al., 2013; Jayasankar et al., 2015; Sharmila et al., 2015; Kitoh, 2017).

The capabilities of climate models in simulating the Indian monsoon have improved over time, such that more accurate projections can be expected from the latest update of the climate models in CMIP-6. Several studies found a broad range of

improvements between CMIP-3 and CMIP-5 in simulating the 20th century monsoon (Sperber et al., 2013; Ogata et al., 2014; Ramesh and Goswami, 2014) though one study, based on a small subset of models, however, disagrees (Shashikanth et al., 2014). Gusain et al. (2020) found a significant improvement between CMIP-5 and CMIP-6 in simulating the Indian summer monsoon rainfall for the period 1951-2005. Models in CMIP-5 still struggled with various issues including displaying the decrease in rainfall in the second half of the 20th century (Saha et al., 2014; Sabeerali et al., 2015; Ashfaq et al., 2017), capturing observed trends in the extremes (Mishra et al., 2014a) and seasonality indices (Ul Hasson et al., 2016). With the new generation, models' capacities in capturing the spatiotemporal pattern of Indian summer monsoon, especially in the Western Ghats and the North-East foothills of Himalaya mountains, have undergone significant progress (Gusain et al., 2020). While global coupled models in CMIP-5 failed to capture the influence of topography, land-surface-feedback and land use change due to their coarse spatial resolution, the general higher resolution in CMIP-6 contributes to an improved simulation of Indian monsoon dynamics (Singh et al., 2019; Gusain et al., 2020). Further improvements have been achieved by updating deep convective schemes, modifying parameterization on microphysical scale, integrating indirect effects of aerosols in cloud formation and advancing ocean-ice models (Gusain et al., 2020).

Here, we aim to update the CMIP projections for the Indian monsoon rainfall and its interannual variability for the 21st century by using 32 models of the latest climate model generation. For this purpose, we use the shared socioeconomic pathways and possible corresponding forcing levels as scenario framework (O'Neill et al., 2017). Section 2 gives a brief overview of the data used and processed. In section 3.1 we evaluate the participating models according to their capacity of modeling the Indian summer monsoon in historic periods. Section 3.2 presents the results of the mean summer monsoon precipitation while section 3.3 focuses on the long-term trend of interannual variability. The results are discussed in section 4.

2   Data and methods

In this study, we investigate the mean Indian summer monsoon rainfall and its interannual variability under four different scenarios using 32 global climate models that participated in CMIP-6. The four scenarios (SSP1-2.6, SSP2-4.5, SSP3-7.0 and SSP5-8.5) are based on different socio-economic scenarios and combined with the resultant forcing level (Van Vuuren et al., 2014; O'Neill et al., 2017). The models are chosen according to their data availability for the historic period (1850-2015) and the future period (2015-2100) under SSP5-8.5 in ScenarioMIP (Tebaldi et al., 2020). For each model, for consistency, we use one ensemble member (if available: r1i1p1f1) even if more are available. An overview of modeling centers and data availability for the different scenarios is given in Table 1. The short names of the models used in this study can be found in Table 2. We select the land area with longitude 67.5°E-98°E and latitude 6°N-36°N, comprising India and neighboring regions. The land area is obtained by using land-sea-masks for each model that are based on the percentage of the grid cells occupied by land (see Fig. 3 for each model). The resolution strongly differs between the models ranging over land from about 100 km to 500 km (see Table 2). Mean rainfall is obtained by averaging the monthly rainfall data from June-September over the region of interest. For comparison of models to observational data, we use precipitation over land from global reanalysis data at 0.5° spatial resolution. The WFDE5 dataset (Cucchi et al., 2020) is used for the period 1985-2015, while for the pre-satellite

era period 1900-1930, we use the GSWP3 dataset (Kim, 2017). Both datasets are based on Global Precipitation Climatology Centre (GPCC) monthly precipitation rates (Schneider et al., 2018; Lange, 2019). For calculating the change in interannual variability, we apply the Singular Spectrum Analysis Method (Golyandina and Zhigljavsky, 2013) with a window size of 20 years to extract the nonlinear trend.

3 Results

3.1 Model comparison

To evaluate the models' quantitative capacities of capturing the Indian monsoon rainfall, we compare their projected seasonal mean rainfall with WFDE5 reanalysis data over land (Cucchi et al., 2020) for two 30-year-periods in the past (1900-1930, 1985-2015). We choose these periods to obtain a model evaluation for a historic period as well as for a period close to present. The seasonal mean rainfall from the reanalysis data is 6.1 mm/day with a standard deviation of 0.5 mm/day for 1900-1930 and 6.1 ± 0.4 mm/day for 1985-2015 (Fig. 1). For both periods, about half of the models capture the quantitative JJAS rainfall within twice the standard deviation (dashed lines in Fig. 1). The standard deviation of the models ranges from 0.3 to 0.8 mm/day for 1900-1930 and 0.3 to 1.0 mm/day in 1985-2015 (error bars in Fig. 1). The models INM-CM4-8 and FIO-ESM-2-0 overestimate the annual rainfall for both periods, the mean value of BCC-CSM2-MR exceeds the upper threshold in 1985-2015. Several models underestimate the seasonal mean rainfall, especially the models of the Canadian Centre for Climate Modeling and Analysis (CanESM5-CanOE, CanESM5) which capture just about half of the reanalysis rainfall amount. All models that underestimate the rainfall for 1900-1930 show rainfall means below the lower threshold in 1985-2015, too. GFDL-CM4 for 1900-1930 and GISS-E2-1-G for 1985-2015 capture the seasonal rainfall quantitatively best. The other models that are closest to the reanalysis mean overlap for both periods, e.g. CNRM-CM6-1, NorESM2-MM and FGOALS-f3-L. For the two chosen time periods, models that capture, over- or underestimate the mean rainfall within twice the standard deviation mostly have the same tendency for both periods. The multi-model mean for 1900-1930 is 5.6 ± 1.1 mm/day and 5.7 ± 1.1 mm/day for 1985-2015.

   In order to identify models with a potentially realistic representation of the Indian monsoon rainfall, we also analyze the spatial precipitation distribution for 1985-2015. We choose this period since it is closer to present time and therefore closer to the simulated time period in the future. As reference data set we use WFDE5 reanalysis data again. The distribution is dominated by rainfall over the Western Ghats, the Himalaya region, the west coast of the Bay of Bengal, the northeast of India and the north of Myanmar partly even exceeding 20 mm/day averaged over JJAS and the 30 year period. The east of central India reaches rainfall values above 10 mm/day (Fig. 2). The spatial rainfall pattern for the CMIP-6 models in 1985-2015 is shown in Fig. 3. Models that captured the rainfall quantitatively well mostly simulate a spatial pattern close to the reference distribution e.g. NorESM2-MM, CNRM-CM6-1, FGOALS-f3-L. FIO-ESM-2-0 overestimates the rainfall in the Himalaya region. The models with the tendency to underestimate the rainfall as ACCESS-CM2, CanESM5-CanOE, CanESM5 mostly are not able to capture the spatial pattern. Especially the southwest coast of India and the Himalaya region are not reproduced
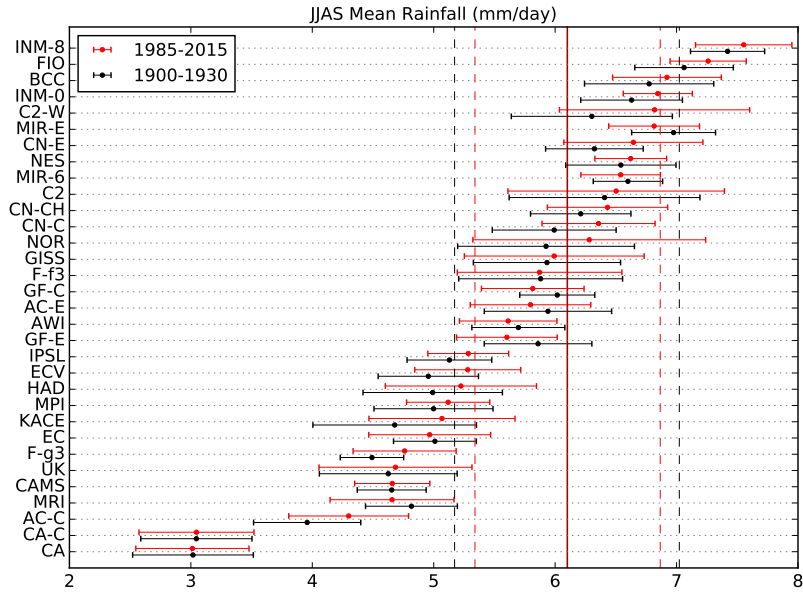
Figure 1. Indian summer monsoon mean rainfall (mm/day) over the region displayed in Fig.3 from 32 different models for the period 1985-2015 (red) and 1900-1930 (black). The vertical line represents the mean monsoon rainfall from WFDE5 reanalysis data for the same periods, the dashed lines show plus/minus twice the standard deviation across the 30-year time period. Circles with error bars represent mean and mean plus/minus one standard deviation for each CMIP-6 model in the same region and the same period.

according to the reanalysis data by most of these models. An exemption for the models with low rainfall values are the models of EC-Earth-Consortium (EC-Earth3, EC-Earth3-Veg) which simulate a pattern very close to the reference distribution.

160   For presenting and discussing the results of this study, we decided to focus on the models within mean plus/minus twice the standard deviation which also deliver a reasonable spatial rainfall pattern. Nevertheless, we will provide information for all 32 models.

3.2   Trend in Indian summer monsoon mean rainfall for the end of the 21st century

In order to determine the long-term trend in Indian monsoon rainfall, we first analyze the temporal time series between 1850-
165   2100 for all models under SSP5-8.5 (Fig. 4). All available models show a clear positive long-term trend. The models exceed the envelope of the baselines variability (grey vertical lines in Fig. 4) between 2014 (HadGEM3-GC31-LL) and 2088 (CESM2), on average over all models in 2045. For the other SSPs, the evolution in time as well as the magnitude of change by the end of the 21st century is indicated as model mean in Fig. 5.

To analyze the change in mean seasonal rainfall until the end of the 21st century, we calculate the difference between the
170   periods 2070-2100 and 1985-2015 for the four SSPs. In the stronger forced scenarios (SSP3-7.0 and SSP5-8.5), all models project an increase of precipitation. In the scenarios with less forcing (SSP1-2.6 and SSP2-4.5), the clear majority of models
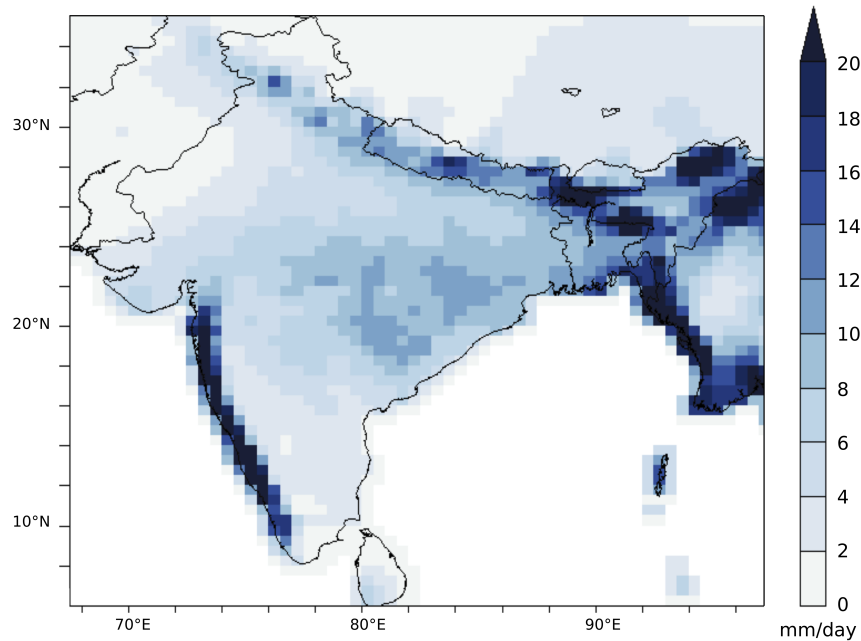
Figure 2. Spatial distribution of Indian summer monsoon rainfall (mm/day) averaged over the period 1985-2015 from WFDE5 reanalysis data.

project an increasing trend, too. The only models to project a decrease are the models of the National Center for Atmospheric Research (CESM2-WACCM in SSP1-2.5 and SSP2-4.5 and CESM2 in SSP2-4.5). On average over all models an increase of 24,3% is projected under SSP5-8.5 (Fig. 6) and of +18,6% in SSP3-7.0 (Appendix Fig. A1), of +11,9% in SSP2-4.5 (Appendix Fig. B1) and of +9.7% in SSP1-2.6 (Appendix Fig. C1). CanESM5 and CanESM5-CanOE show the maximum relative increase in all scenarios by the end of the 21st century. But as shown in Fig. 1 and Fig. 3, they clearly underestimate the rainfall and do not capture a realistic pattern of the rainfall distribution. CESM2-WACCM shows the minimal increase of 7.8% under SSP5-8.5. This model was able to capture the mean rainfall in 1985-2015 within twice the standard deviation and is able to capture a reasonable pattern of the rainfall. Focusing on the models that captured the mean rainfall in 1985-2015 within twice the standard deviation (upper panel in Fig. 6), the relative increase is 17.4% under SSP5-8.5, i.e. slightly less than the average over all models. Also in the other scenarios the trend is less for these models compared to the average over all models. In summary, a robust increase of seasonal rainfall between 1985-2015 and 2070-2100 can be derived under global warming.

Most models project that this increase will contribute to the precipitation especially in the Himalaya region and to the northeast of the Bay of Bengal, as well as the Western Ghats (Fig. 7). Individual models indicate decreasing rainfall along the southwest coast of India and around Myanmar.

Furthermore, we analyzed the dependence of rainfall on global mean temperature (GMT, Fig. 8). The simulation ensemble indicates a linear dependence of rainfall on GMT, with a high agreement between models and independent of the scenarios if global warming is the dominant forcing of the monsoon dynamics as it is in the 21st century. The multi-model mean indicates
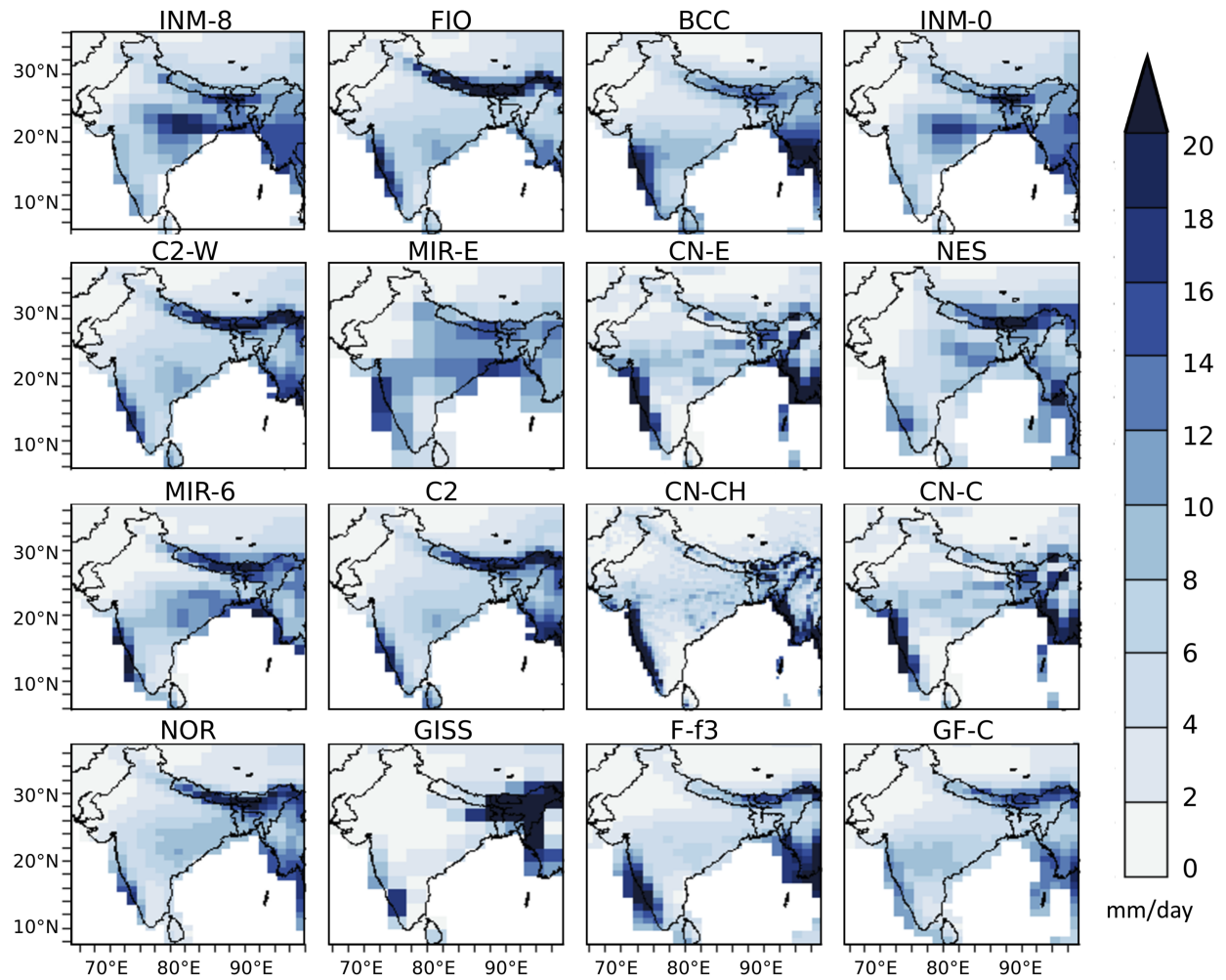
Figure 3. Spatial distribution of Indian summer monsoon mean rainfall (mm/day) averaged over the period 1985-2015. The models are shown in the same order as in Fig. 1.
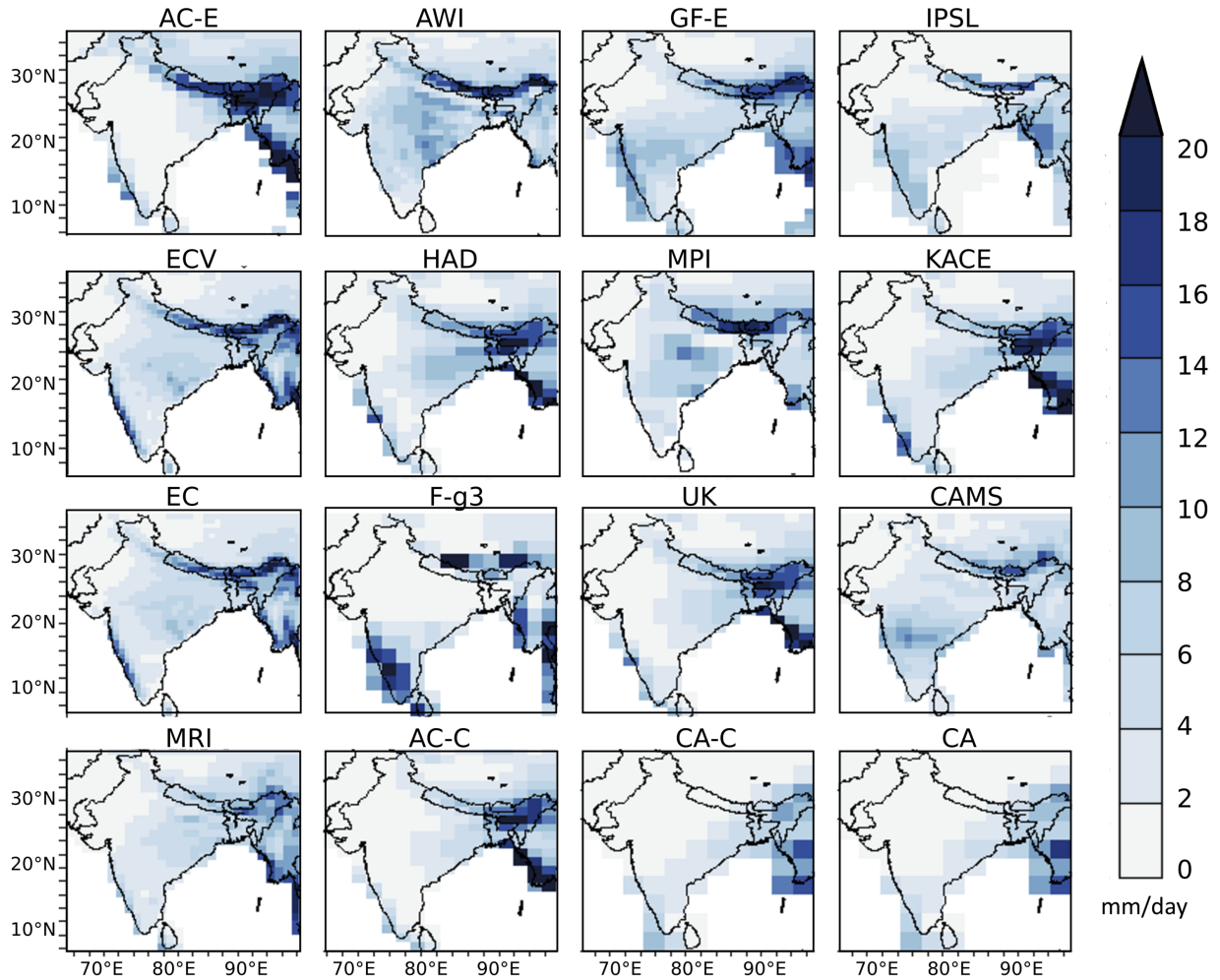
Figure 3 (continued).

an increase of 0.33 mm/day ranging from 0.11 mm/day to 0.54 mm/day. The relative dependence is 5.3% per degree of global warming ranging from 1.7%/K to 13.4%/K for SSP5-8.5 across models. Considering only the more realistic models, the projected mean change is 6.1%/K for SSP5-8.5.

3.3   Long-term trend of interannual variability

In order to analyze the future evolution of interannual variability, we removed the nonlinear trend obtained by a Singular Spectrum Analysis from the rainfall data as displayed in Fig. 4, and use the percentage changes in standard deviation for the period 2050-2100 with respect to 1900-1950. Under SSP5-8.5, 28 of 32 models indicate an increase of interannual variability (Fig. 9); the multi-model mean in this scenario indicates an increase of 21.3%. The strongest increase of 56.2% is simulated
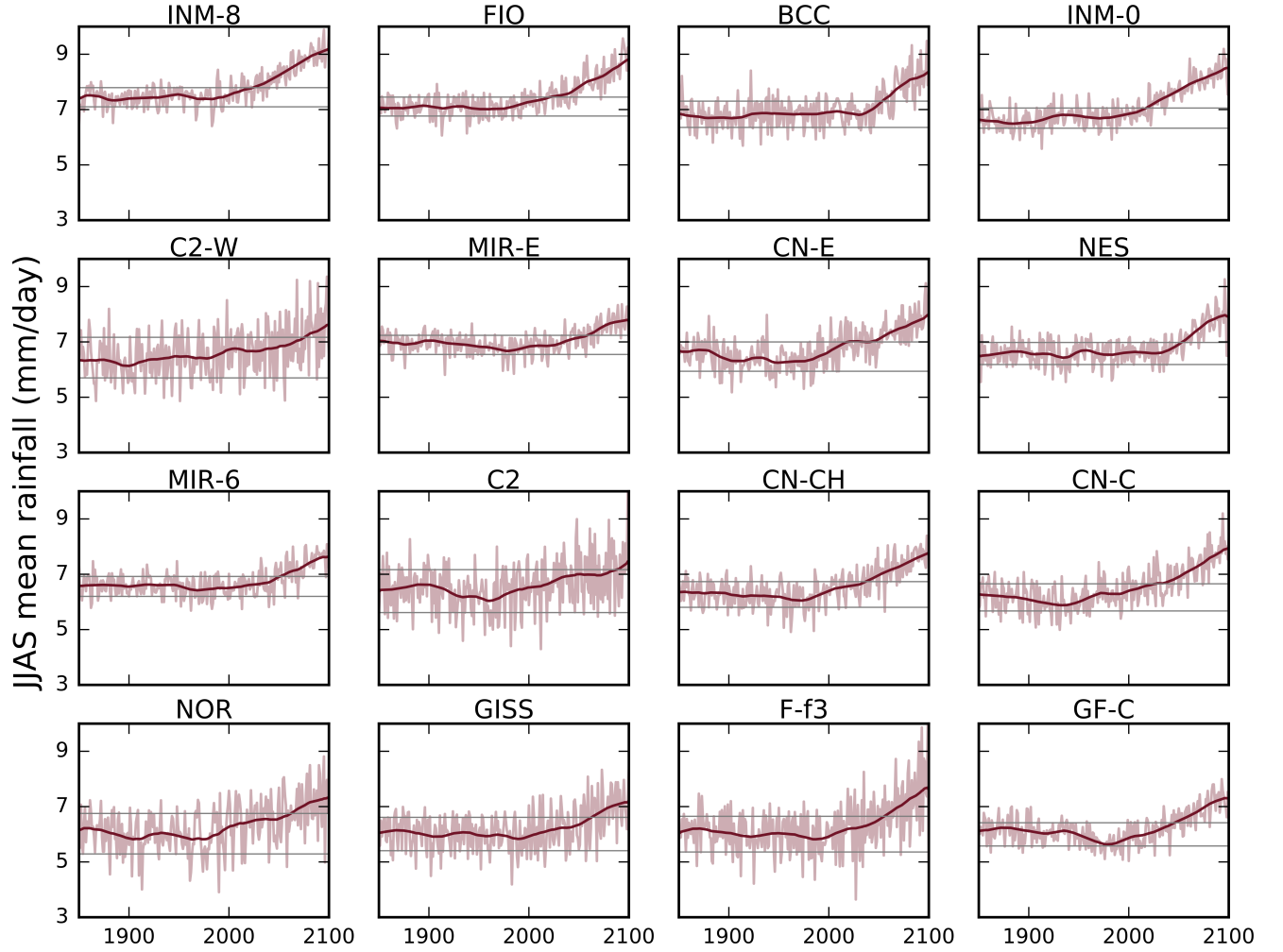
Figure 4. Time series of Indian summer monsoon mean rainfall (mm/day) for the period 1850-2100 from the 32 climate models under SSP5-8.5. The underlying area is according to the displayed region in Fig. 3. Red shadings represent the yearly values, red lines represent the nonlinear trend obtained from a Singular Spectrum Analysis with a window size of 20 years according to the method from Golyandina and Zhigljavsky (2013). The horizontal black lines represent mean plus/minus standard deviation for each model for the period 1850-2015. The order is according to Fig. 1. For the multi-model mean under SSP5-8.5 and other scenarios refer to Fig. 5.
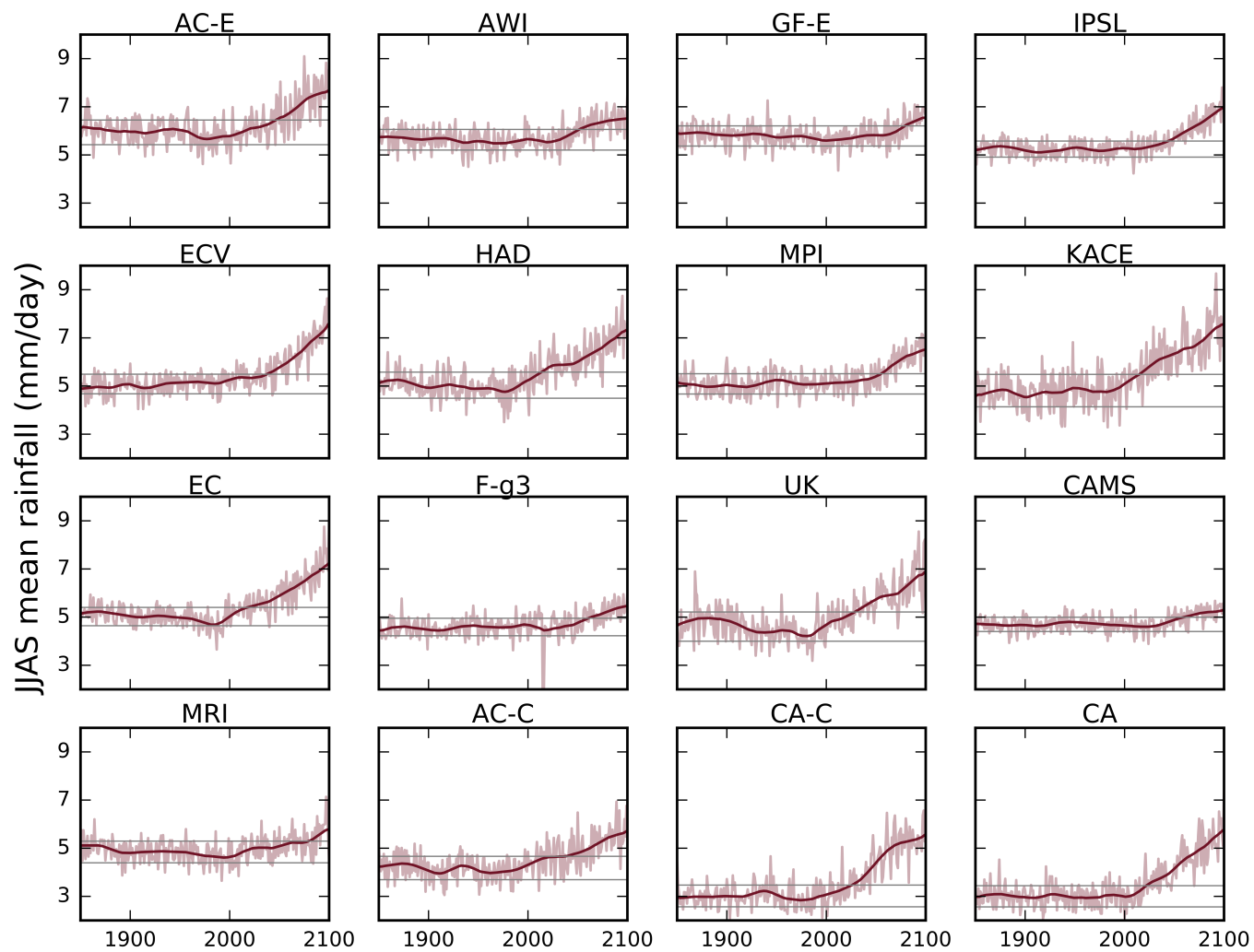
Figure 4 (continued).
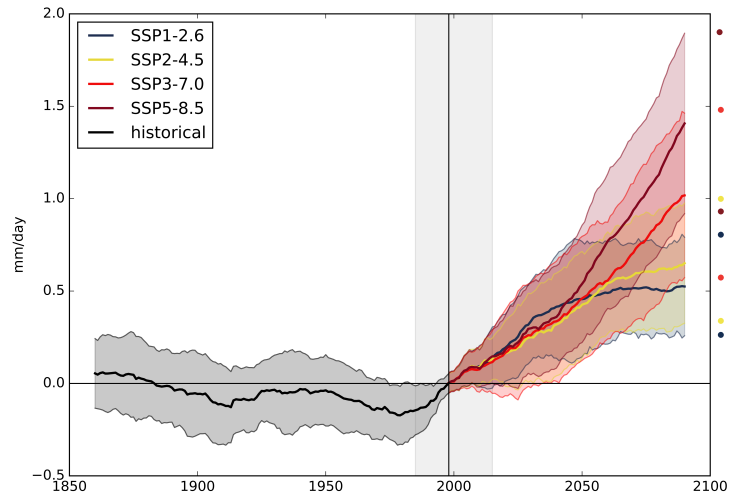
Figure 5. Multi-model mean of Indian summer monsoon rainfall (mm/day) over displayed area in Fig. 3 for 1860-2090 relative to the mean (horizontal black line) in 1985-2015 (grey background) for the four scenarios SSP1-2.6, SSP2-4.5, SSP3-7.0 and SSP5-8.5. The 20 years smoothed time series of one ensemble member per model was used to calculate the multi-model mean. Shading in the time series represents the range of mean plus/minus one standard deviation marked with circles on the right sight of the Figure. Availability of the models according to Table 1.

by EC-Earth3-Veg which is a model that does not capture the quantitative rainfall of the Indian summer monsoon well. Four models simulate a decrease in SSP5-8.5: Both models from INM (INM-CM4-8, INM-CM5-0) and two models from CNRM-CERFACS (CNRM-CM6-1-HR, CNRM-ESM2-1) project a decrease in interannual variability. Even if two of the four models

200 projecting a decrease under SSP5-8.5 show a relatively small decrease of less than 5%, it has to be noted that all of this four but INM-CM4-8 captured the rainfall in 1985-2015 within twice the standard deviation, making them more reliable in projecting the Indian summer monsoon than some other models. Nevertheless, among the 16 models within twice the standard deviation, 13 project an increase in interannual variability. In SSP3-7.0, 22 out of the available 27 models project an increase of interannual variability (See Appendix Fig D1). The signal in the scenarios with less forcing is less clear (See Appendix

205 Fig. E1 and Fig. F1), but even in SSP1-2.6 still 21 out of 31 available models project an increase in interannual variability until the second half of the 21st century. For the purpose of comparison, we also calculated the change without removing the trend and found that for SSP5-8.5 all models project an increase in interannual variability in average 39.9%. Fig. 10 shows the dependence of interannual variability on global mean temperature for all available models (after removing the trend). As the global mean temperature change grows with stronger forcing, the positive trend in interannual variability becomes clearer.
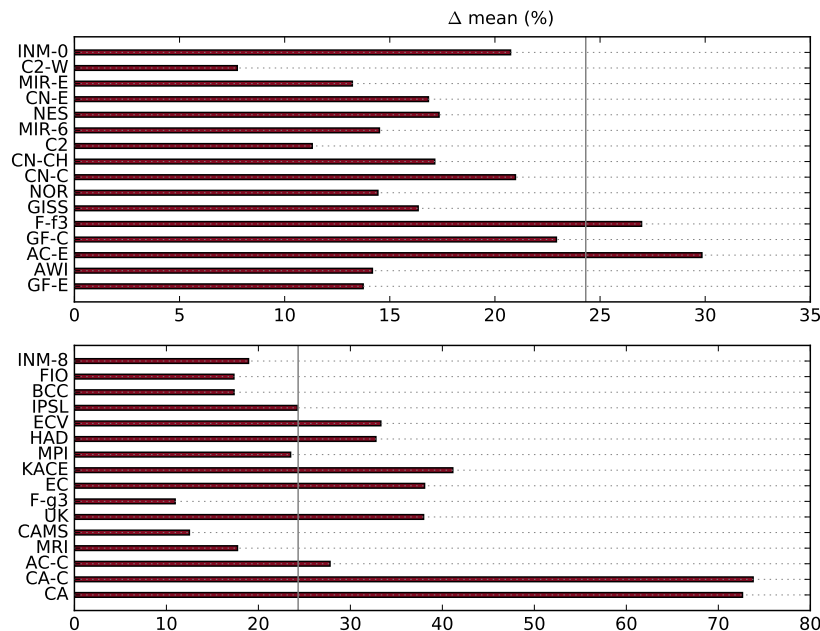
Figure 6. Percentage change in Indian summer monsoon mean rainfall for SSP5-8.5 for all 32 models over the area displayed in Fig. 3. Relative change is calculated as the change in mean rainfall for the period 2070-2100 with respect to the period 1985-2015. The gap separates models with rainfall values for 1985-2015 within twice the standard deviation of the reanalysis mean as in Fig. 1 from those outside that range. Please notice the different scales in the two panels. The mean over all models is +24.3% (vertical grey line).

4   Discussion

In this study, the long-term trend of the Indian summer monsoon and its variability have been analyzed based on the latest global coupled model simulations under the SSP scenarios. Our approach addresses the question whether the results from earlier studies can be confirmed or need to be adapted in their sign or magnitude.

By comparing the CMIP-6 projection results with the WFDE5 reanalysis data, we classified some models as probably more capable of simulating a realistic representation of the monsoon rainfall. The share of models that capture the reference rainfall within twice the standard deviation has slightly increased in CMIP-6 (16 out of 32) in comparison to the precursor models in CMIP-5 (9 out of 20) (Menon et al., 2013). But it has to be noted that the validation period and the used reanalysis data differ between (Menon et al., 2013) and this study. The observation of quantitatively measurable improvement between CMIP-5 and CMIP-6 coincides with the results of Gusain et al. (2020). While all the models that were out of the two standard deviation range underestimated the mean in CMIP-5, thus revealing a very clear general tendency of underestimation, the 16 models outside of the range in CMIP-6 partly underestimated (13 models) and party overestimated (3 models) the observed mean in 1985-2015. Modeling centers whose models underestimated the rainfall within two standard deviations in our study mostly underestimated the rainfall already in CMIP-5. Some models with realistic patterns in CMIP-6 are updates from CMIP-5 that
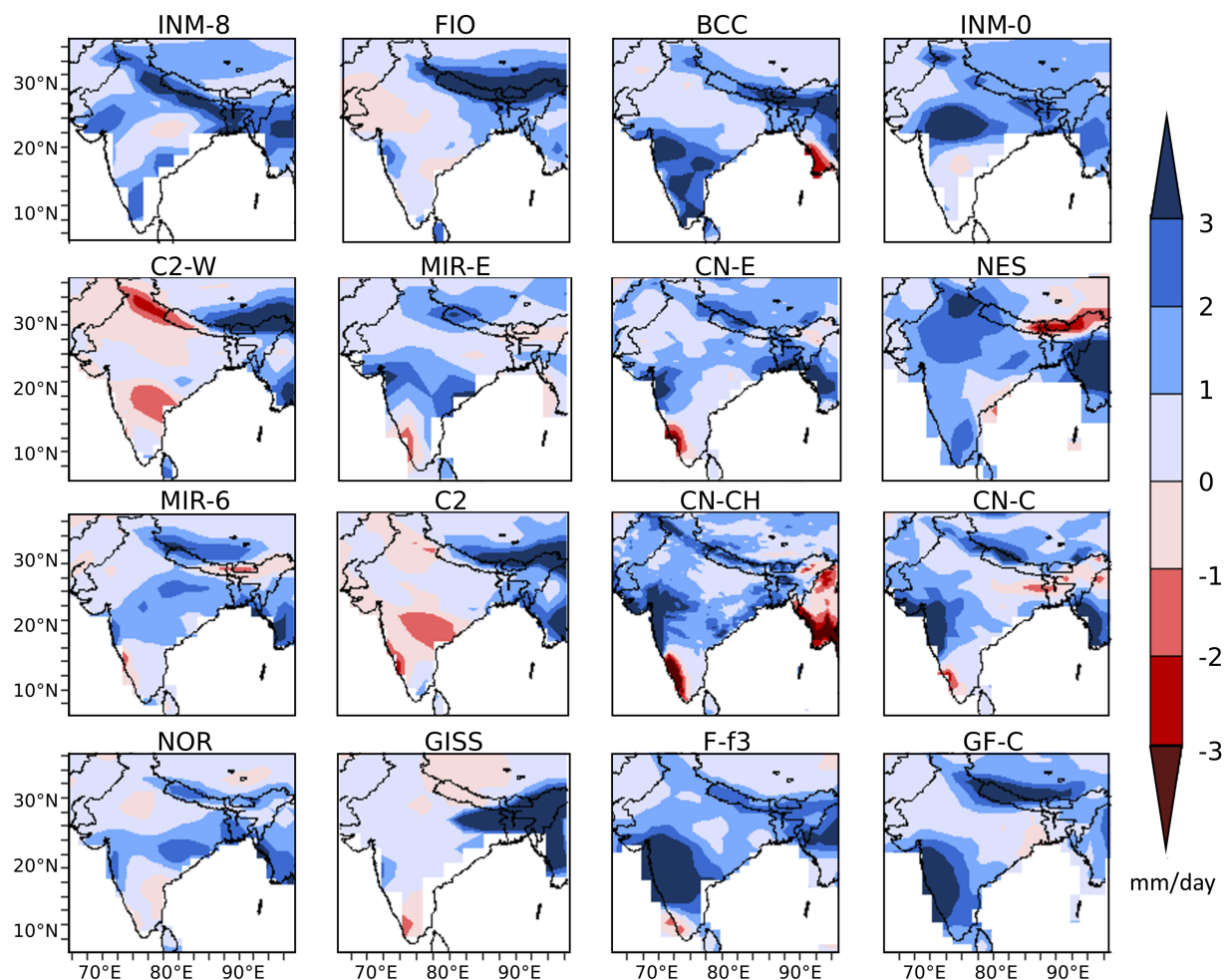
Figure 7. Difference in Indian summer monsoon mean rainfall (mm/day) for the period 2070-2100 under SSP5-8.5 in comparison to 1985-2015.

already revealed a pattern relatively similar to reanalysis data, e.g. NorESM2-MM. As in CMIP-5, models with the tendency to underestimate the rainfall in the evaluation period are mostly not capable either of capturing the spatial rainfall pattern in CMIP-6. But there are also various models that improved their capacity in capturing the Indian monsoon, such as the models from Centre National de Recherches Météorologiques (CNRM-CM6-1, CNRM-CM6-1-HR, CNRM-ESM2-1). This observed inconsistency among models in improving their spatial representation of the Indian monsoon was already noted by Gusain et al. (2020). Besides, the capacity of capturing the rainfall pattern over the Western Ghats has improved what also coincides with the results of (Gusain et al., 2020).

The CMIP-6 models project a robust intensification of the Indian summer monsoon rainfall under climate change. All of the 32 available models exceed the envelope of baseline variability from 1850-2015 until 2100 under SSP5-8.5, while just
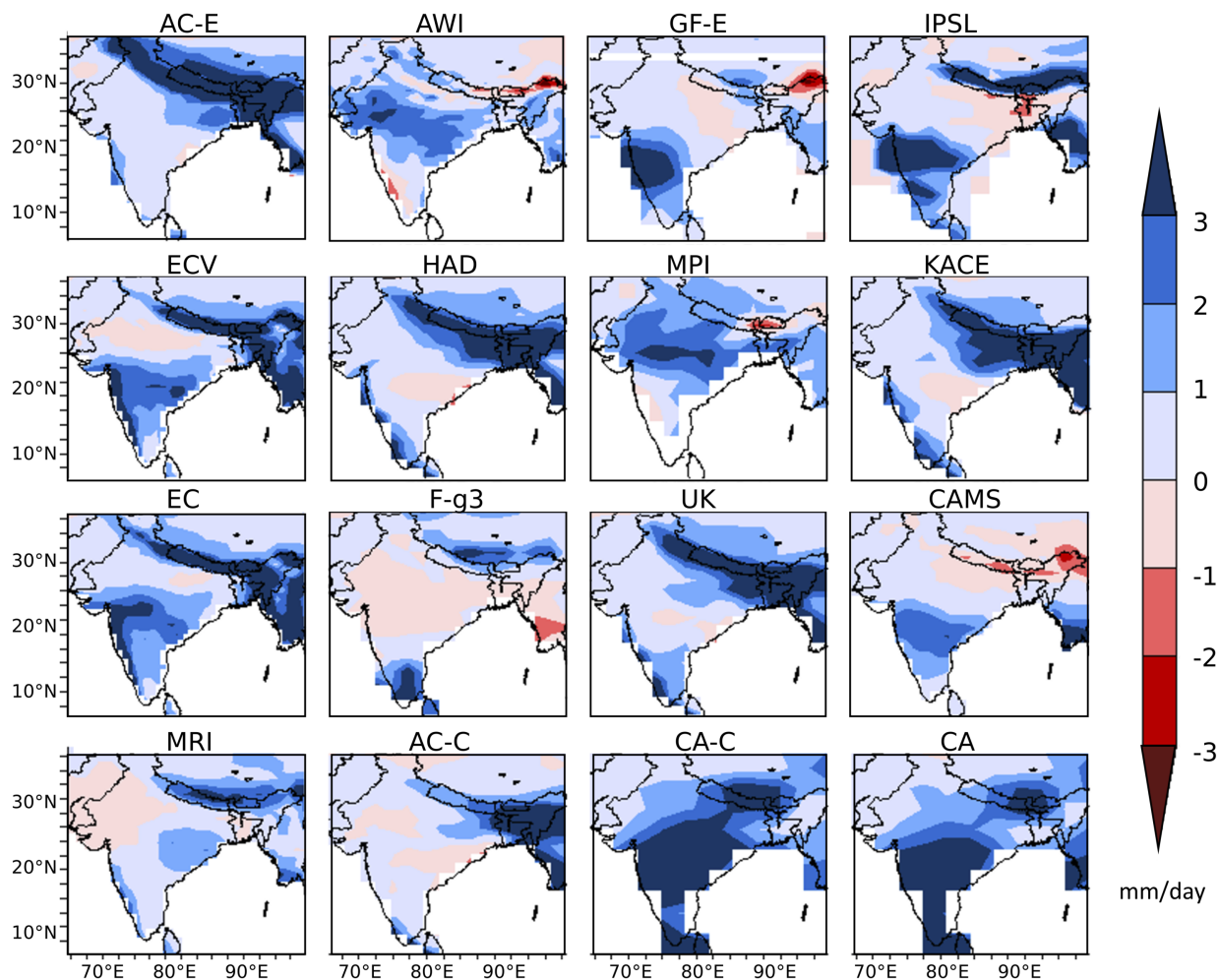
Figure 7 (continued).

17 out of 20 exceeded the natural variability threshold under RCP-8.5 in a previous study based on CMIP-5 (Menon et al., 2013). Additionally, we calculated the average multi-model trend of projected change in mean rainfall by the end of the 21st century. As some modeling centers provide several models and some of them are based on overlapping model components, the models cannot be regarded as independent from each other (See e.g., Knutti et al., 2017). The results have to be interpreted against this background. The found average multi-model trend in CMIP-6 with an increase of +24.3% by 2100 seems stronger in comparison to CMIP-5 (Chaturvedi et al., 2012; Menon et al., 2013).

Chaturvedi et al. (2012) found an increase of 18.7% in RCP-8.5 by 2099 compared to the period 1961-1990 in CMIP-5 models. But because of the used time periods as well as the different study area of India without adjacent regions, this study is not directly comparable to ours. An intensification of the Indian monsoon rainfall also has been found in other studies using CMIP-5 (Lee and Wang, 2014; Mei et al., 2015; Sharmila et al., 2015; Varghese et al., 2020). There is a widespread agreement
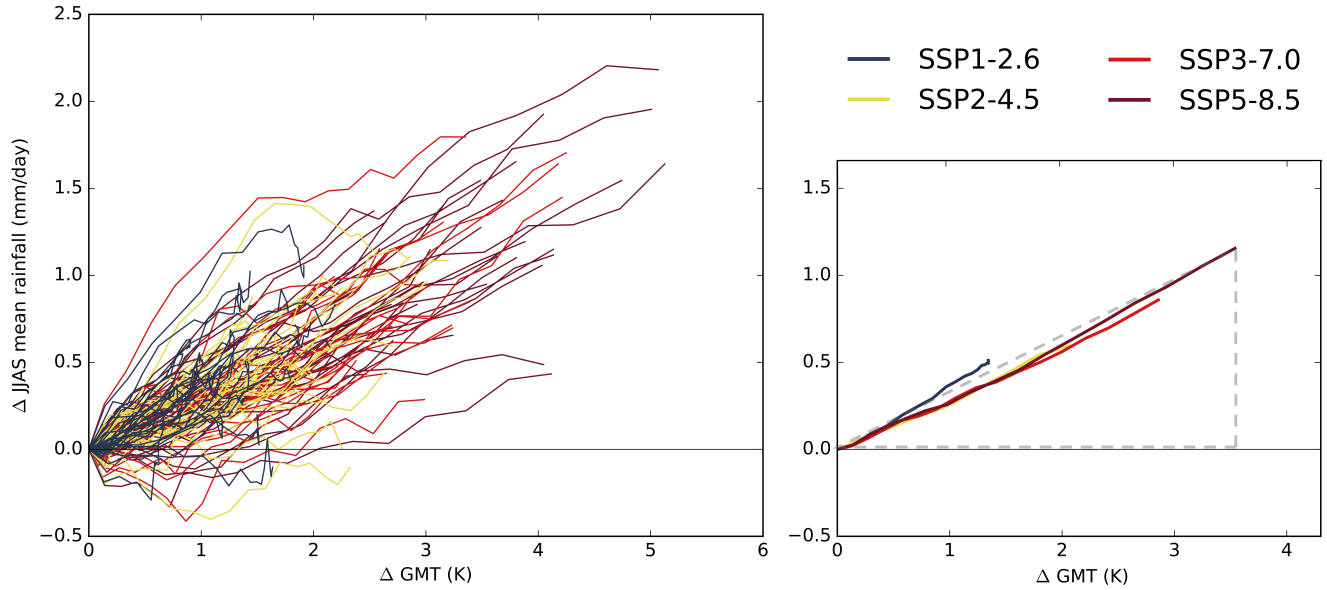
Figure 8. Change of Indian summer monsoon mean rainfall (mm/day) depending on change in global mean temperature (K) until the end of the 21st century relative to the period 1985-2015 for four scenarios. Underlying regions as in Fig. 3. Means are calculated over decadal periods starting in 2005 and overlapped by five years (2005-2014, 2010-2019, up to 2090-2099). Left: Each line represents a different model (one ensemble member per model). Right: Each line represents multi-model mean for one scenario. Model availability for global temperature in different scenarios can be seen in Table 1. Grey dashed lines indicate the slope (the hydrological sensitivity) for SSP5-8.5

that a reason for the intensification of the South Asian monsoon rainfall is an increase in moisture flux convergence (Singh et al., 2019). This enhanced thermodynamic effect dominates over the dynamic effect which refers to the decreasing monsoon

245 circulation. D'Agostino et al. (2019) quantified the increase of the thermodynamic component of the moisture budget for the Indian monsoon with about 0.7mm/day and the decrease of the dynamic component with 0.4mm/day using nine CMIP-5 models in RCP-8.5 determining the positive sign of the change in monsoon rainfall (D'Agostino et al., 2019; Sooraj et al., 2015).

We found that the monsoon rainfall is linearly dependent on the GMT. This is not in contradiction with the observed decline

250 in monsoon rainfall during the second half of the 20th century: While between the 1950s and 70s, approximately, high aerosol loadings led to subdued warming and a weakened land-sea thermal gradient, greenhouse gas-induced warming has dominated since then and is the dominant forcing in the 21st century projections. The projected increase in rainfall is 0.33 mm/day per degree of global warming. The agreement between models and the independence of the scenario is remarkable. The median dependence of relative change in precipitation on GMT taking into account all models has increased from 3.2%/K in CMIP-

255 5 to 5.3%/K in CMIP-6. Considering only the models with a more realistic representation of the monsoon, the increase is even more noticeably from 2.3%/K in CMIP-5 to 6.1%/K in CMIP-6. It also has to be mentioned that the range of projected sensitivities has decreased remarkably from 1-19%/K in CMIP-5 to 2-13%/K in the latest generation of climate models, i.e.
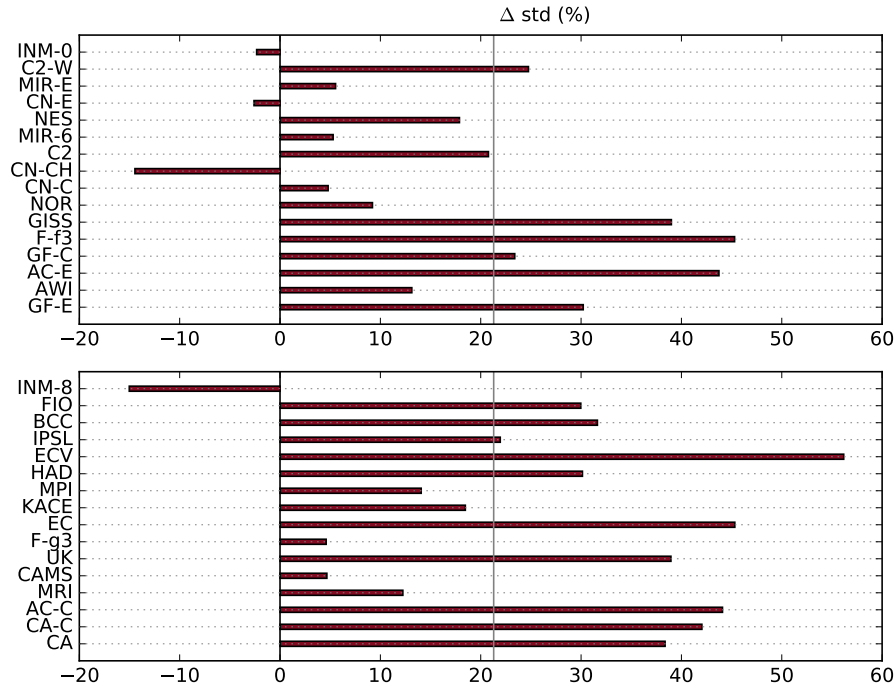
Figure 9. The percentage change of standard deviation between the second half of the 21st century to the standard deviation from 1900-1950 under SSP5-8.5. For the underlying area refer to Fig. 3. We used a Singular Spectrum Analysis algorithm (Golyandina and Zhigljavsky, 2013) to remove the nonlinear trend according to Fig. 4. The mean percentage change in this scenario is 21.3 %. The gap separates models as in Fig. 1 according to their capacity of capturing the monsoon rainfall in 1985-2015.

the uncertainty in hydrological sensitivity has decreased with the model updates. Similar tendencies have been found for the equilibrium climate sensitivity in CMIP-6 Zelinka et al. (2020); Wyser et al. (2020). Which of the updated processes between CMIP-5 and CMIP-6 described by Gusain et al. (2020) dominate in causing the increased sensitivity of the monsoon to global warming needs further investigation.

The increase in rainfall is projected to contribute to the precipitation in the Himalaya region, the northeast Bay of Bengal and the northwest coast of India. These regions coincide to a large extent with the existing monsoon rainfall pattern, leading to a wet regions get wetter pattern during June to September monsoon rainfall. The distribution of regions with projected increasing precipitation in CMIP-6 confirms the projection of previous studies using CMIP-5 models (Chaturvedi et al., 2012; Menon et al., 2013; Sharmila et al., 2015). Furthermore, the increasing pattern is shared by a larger percentage of available models in CMIP-6 compared to CMIP-5. But our projection of increased rainfall over the Western Ghats does not coincide with the study of Varghese et al. (2020) projecting a decrease in this region. By focusing on high resolution models with the best deep convection scheme, their study reveals decreasing precipitation in the southwest coast of India, which is only captured by one
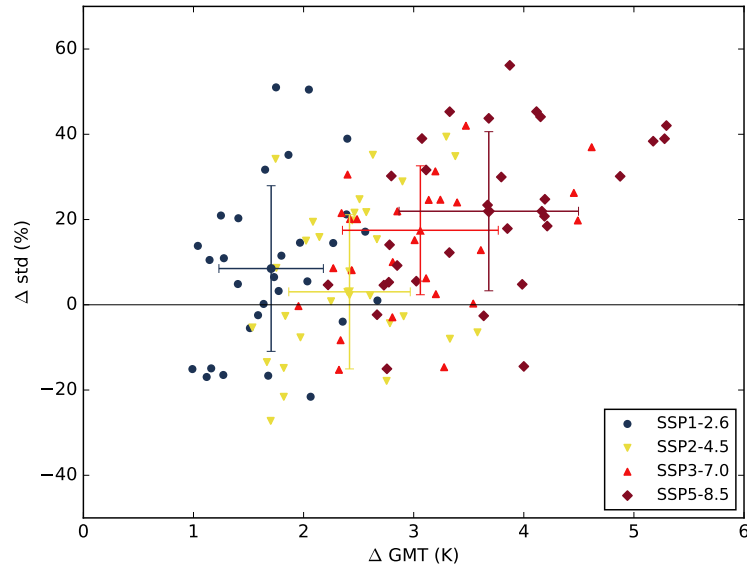
Figure 10. Scatterplot of percent change in standard deviation(%) and change in global mean temperature (K) between 2050-2100 and 1950-2000 for four scenarios. The symbols with error range represent the median plus/minus the standard deviation in each scenario. The underlying area can be seen in Fig. 3. The trend was removed before using a Singular Spectrum Analysis algorithm (Golyandina and Zhigljavsky, 2013). Availability of models for different scenarios can be seen in Table 1.

270 third of the CMIP-6 models in our study, including the CNRM-CM6-1-HR model. A finer resolution seems to be necessary to capture this trend which is not given for all CMIP-6 models.

From the 32 available models, 28 models project an increase in interannual variability. This result is not directly comparable to the study of Menon et al. (2013) since the removal of the trend in our study has a relevant influence on the results. Without the removal of the trend, i.e. following the method of Menon et al. (2013), all 32 models project an increase in interannual

275 variability which shows that the signal has become clearer in comparison to the results in CMIP-5 models. The projected increase in interannual variability coincides with other studies (Kitoh et al., 1997; Jayasankar et al., 2015; Sharmila et al., 2015; Kitoh, 2017). A dominant role in shaping the interannual variability is taken by the El Niño Southern oscillation (ENSO) (Turner and Annamalai, 2012). As El-Niño events typically coincide with dry monsoon years and La-Niña years are often accompanied by strong monsoon rainfall (Kumar et al., 2006), changes in the emergence of these events have a relevant impact

280 on the Indian summer monsoon. (Azad and Rajeevan, 2016) applied spectral analysis and found a shortening of the spectral periods of ENSO which might lead to a shift in the relationship of ENSO and monsoon rainfall.

5   Conclusion

We used 32 CMIP-6 models to analyse the Indian summer monsoon's response to climate change. In order to identify models with a good representation of the Indian monsoon, we compared the models' simulations in the past to WFDE5 reanalysis data. We found that there are 16 out of 32 models that are able to capture the monsoon rainfall within twice the standard deviation in the period 1985-2015. This is a slight increase compared to CMIP-5. The models outside that range in CMIP-6 still have a tendency to underestimate the amount of precipitation in this period. This was already observed in CMIP-5 where all of the models out of the range underestimated the rainfall. In our analysis, we focused on the models with the more realistic representation of the Indian monsoon. We found that all models show an increase in mean summer monsoon rainfall under SSP5-8.5 and SSP3-7.0 by the end of the 21st century. An increase also was found in SSP2-4.5 and SSP1-2.6 by all models apart from two models in SSP2-4.5 and one model in SSP1-2.6. Under SSP5-8.5, the models exceed the envelope of the baselines variability on average in 2045 in SSP5-8.5. An multi-model mean increase of rainfall of 24,3% is projected under SSP5-8.5 and of +18,6% in SSP3-7.0, of +11,9% in SSP2-4.5 and of +9.7% in SSP1-2.6. The majority of models project that that the increase will contribute to the precipitation especially in the Himalaya region, the northeast of the Bay of Bengal and to the west coast of India. Besides, the simulation ensemble indicates a linear dependence of rainfall on global mean temperature independent of the SSP in the 21st century; the multi-model mean for JJAS projects an increase of 0.33mm/day and 5.3% per degree of global warming. Furthermore, under SSP5-8.5 a majority of 28 out of 32 models project an increase in interannual variability by the end of the 21st century after removing the trend with Singular Spectrum Analysis.

We have seen in this study that low resolution models did not capture the spatial pattern of the monsoon rainfall in historic periods well. Small scale topography and its atmosphere feedback influence the rainfall to a relevant extent. Thus, the ongoing effort to improve the resolution of the individual CMIP models should be continued. Since other rainfall features such as extremes and the variability of rainfall on a subseasonal scale are beyond the scope of this study, they need to be analyzed in further studies owing to their high relevance e.g. for high-risk flooding events.

The projected increase in summer monsoon rainfall in combination with the projected longterm increase in interannual variability will be accompanied by an increased number of extremely wet years and potentially more high rainfall events (Turner and Slingo, 2009; Sharmila et al., 2015). While crops need water especially in the initial growing period, high rainfall events during other growing states can harm the plants Revadekar and Preethi (2012). Thus, the projected development might have serious consequences for the agriculture in India and neighbouring regions. Since the change differs from the decreasing tendency in the second half of the 20th century, the development of adaptation strategies for the 21st century is required.

Table 1. Overview of data availability for the 32 models used in the study (precipitation/temperature). Only those models are selected for which data for historic period and SSP5-8.5 was available at the time of the study.

Modeling Center (Group)	Model	SSP1-2.6	SSP2-4.5	SSP3-7.0	SSP5-8.5
Alfred Wegener Institute (AWI)	AWI-CM-1-1-MR	Y/N	Y/N	Y/N	Y/N
Beijing Climate Center, China Meteorological Administration (BCC)	BCC-CSM2-MR	Y/Y	Y/Y	Y/Y	Y/Y
Chinese Academy of Meteorological Sciences (CAMS)	CAMS-CSM1-0	Y/Y	Y/Y	Y/Y	Y/Y
LASG, Institute of Atmospheric Physics, Chinese Academy of Sciences (CAS)	FGOALS-f3-L	Y/Y	Y/Y	Y/Y	Y/Y
	FGOALS-g3	Y/Y	Y/Y	Y/Y	Y/Y
Canadian Centre for Climate Modelling and Analysis (CCCma)	CanESM5	Y/Y	Y/Y	Y/Y	Y/Y
	CanESM5-CanOE	Y/Y	Y/Y	Y/Y	Y/Y
Centre National de Recherches Météorologiques/ Centre Européen de Recherche et Formation Avancées en Calcus Scientifique (CNRM-CERFACS)	CNRM-CM6-1	Y/Y	Y/Y	Y/Y	Y/Y
	CNRM-CM6-1-HR	Y/Y	Y/Y	Y/Y	Y/Y
	CNRM-ESM2-1	Y/Y	Y/Y	Y/Y	Y/Y
Commonwealth Scientific and Industrial Research Organisation (CSIRO)	ACCESS-ESM1-5	Y/Y	Y/Y	Y/Y	Y/Y
Commonwealth Scientific and Industrial Research Organisation, ARC Centre of Excellence for Climate System Science (CSIRO-ARCCSS)	ACCESS-CM2	Y/Y	Y/Y	Y/Y	Y/Y
EC-Earth-Consortium	EC-Earth3	Y/Y	Y/Y	Y/Y	Y/Y
	EC-Earth3-Veg	Y/Y	Y/Y	Y/Y	Y/Y
First Institution of Oceanography (FIO-QLNM)	FIO-ESM-2-0	Y/Y	Y/Y	N/N	Y/Y
Institute of Numerical Mathematics (INM)	INM-CM4-8	Y/Y	Y/Y	Y/Y	Y/Y
	INM-CM5-0	Y/Y	Y/Y	Y/Y	Y/Y
Institut Pierre Simon Laplace (IPSL)	IPSL-CM6A-LR	Y/Y	Y/Y	Y/Y	Y/Y0
Japan Agency for Marine-Earth Science and Technology/ Atmosphere and Ocean Research Institute, University of Tokyo (MIROC)	MIROC6	Y/Y	Y/Y	Y/Y	Y/Y
	MIROC-ES2l	Y/Y	Y/Y	Y/Y	Y/Y
Met Office Hadley Centre (MOHC)	HadGEM3-GC31-LL	Y/Y	Y/Y	N/N	Y/Y
	UKESM1-0-LL	Y/Y	Y/Y	Y/Y	Y/Y
Max Planck Institute for Meteorology (MPI-M)	MPI-ESM1-2-LR	Y/Y	Y/Y	Y/Y	Y/Y
Meteorological Research Institute (MRI)	MRI-ESM2-0	Y/Y	Y/Y	Y/Y	Y/Y
NASA Goddard Institute for Space Studies (NASA-GISS)	GISS-E2-1-G	Y/Y	Y/Y	Y/Y	Y/Y

Modeling Center (Group)	Model	SSP1-2.6	SSP2-4.5	SSP3-7.0	SSP5-8.5
National Center for Atmospheric Research (NCAR)	CESM2	Y/Y	Y/Y	N/N	Y/Y
	CESM2-WACCM	Y/Y	Y/Y	Y/Y	Y/Y
Norwegian Climate Center (NCC)	NorESM2-MM	Y/Y	Y/Y	Y/Y	Y/Y
National Institute of Meteorological Sciences-Korea Met. Administration (NIMS-KMA)	KACE-1-0-G	Y/Y	Y/Y	Y/Y	Y/Y
NOAA Geophysical Fluid Dynamics Laboratory (NOAA-GFDL)	GFDL-CM4	N/N	Y/Y	N/N	Y/Y
	GFDL-ESM4	Y/Y	Y/Y	Y/Y	Y/Y
Nanjing University of Information Science and Technology (NUIST)	NESM3	Y/Y	Y/Y	N/N	Y/Y
	Number of models per scenario	31/30	32/31	27/26	32/31
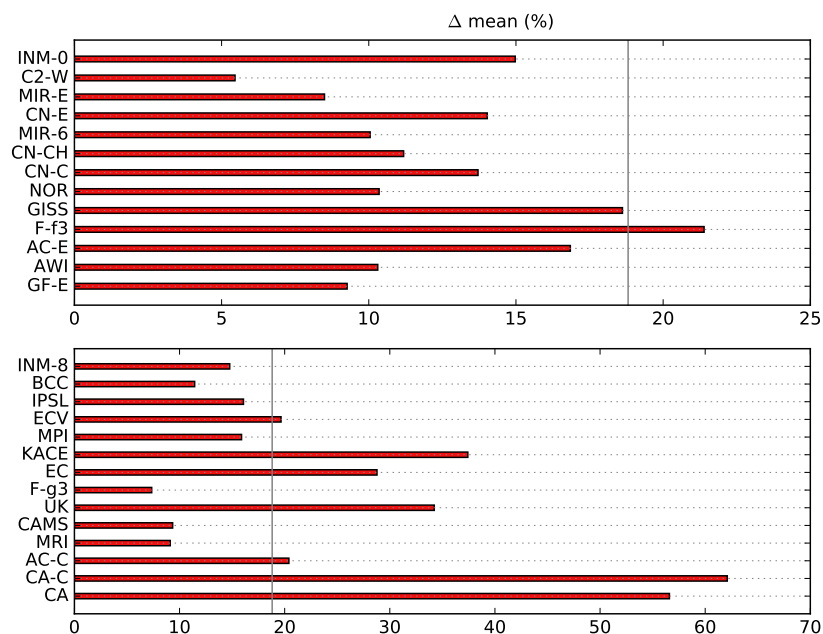
Figure A1. As in Fig. 6 but for SSP3-7.0. The mean over all models is +18.6%. Please notice the different scales in the lower panel.

Table 2. Overview of short names used in this study and resolution in which the 32 models were run.

Model	Short Name	Atmosphere [km]	Land [km]	Ocean [km]
AWI-CM-1-1-MR	AWI	100	100	25
BCC-CSM2-MR	BCC	100	100	50
CAMS-CSM1-0	CAMS	100	100	100
FGOALS-f3-L	F-f3	100	100	100
FGOALS-g3	F-g3	250	250	100
CanESM5	CA	500	500	100
CanESM5-CanOE	CA-C	500	500	100
CNRM-CM6-1	CN-C	250	250	100
CNRM-CM6-1-HR	CN-CH	100	100	25
CNRM-ESM2-1	CN-E	250	250	100
ACCESS-ESM1-5	AC-E	250	250	100
ACCESS-CM2	AC-C	250	250	100
EC-Earth3	EC	100	100	100
EC-Earth3-Veg	ECV	100	100	100
FIO-ESM-2-0	FIO	100	100	100
INM-CM4-8	INM-8	100	100	100
INM-CM5-0	INM-0	100	100	50
IPSL-CM6A-LR	IPSL	250	250	100
MIROC6	MIR6	250	250	100
MIROC-ES2l	MIR-E	500	500	100
HadGEM3-GC31-LL	HAD	250	250	100
UKESM1-0-LL	UK	250	250	100
MPI-ESM1-2-LR	MPI	250	250	250
MRI-ESM2-0	MRI	100	100	100
GISS-E2-1-G	GISS	250	250	100
CESM2	C2	100	100	100
CESM2-WACCM	C2-W	100	100	100
NorESM2-MM	NOR	100	100	100
KACE-1-0-G	KACE	250	250	100
GFDL-CM4	GF-C	100	100	25
GFDL-ESM4	GF-E	100	100	50
NESM3	NES	250	2.5	100
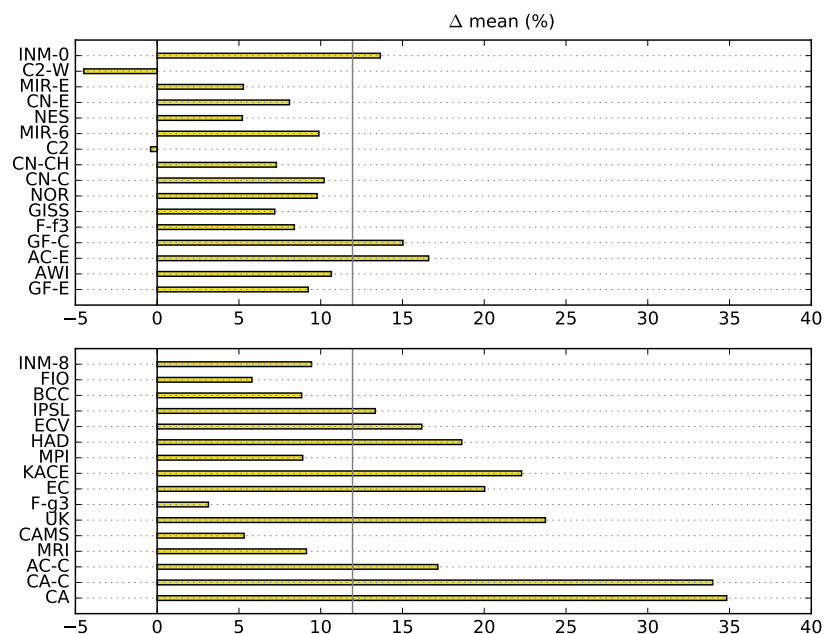
Figure B1. As in Fig. 6 but for SSP2-4.5. The mean over all models is +11.9%
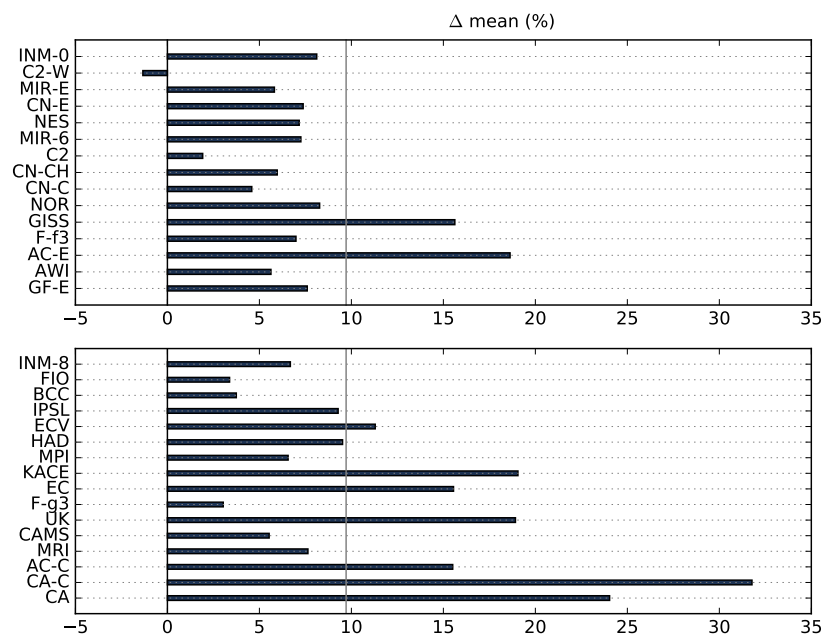
Figure C1. As in Fig. 6 but for SSP1-2.6. The mean over all models is +9.7%
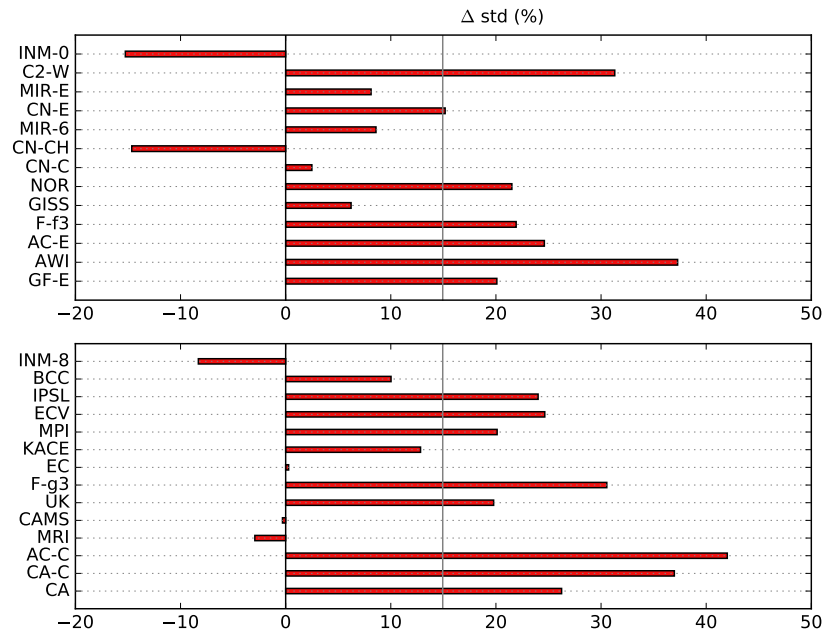
Figure D1. As in Fig. 9 but for SSP3-7.0.
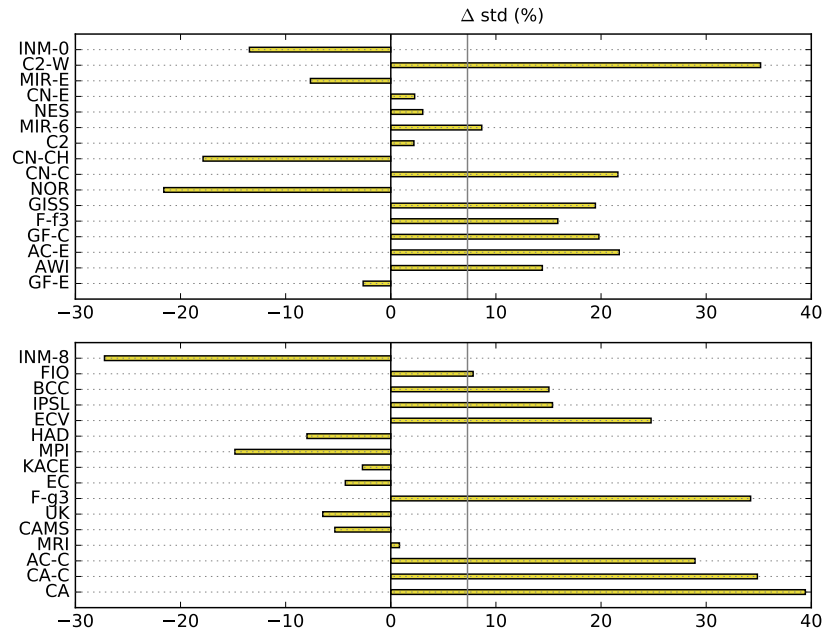
Figure E1. As in Fig. 9 but for SSP2-4.5.
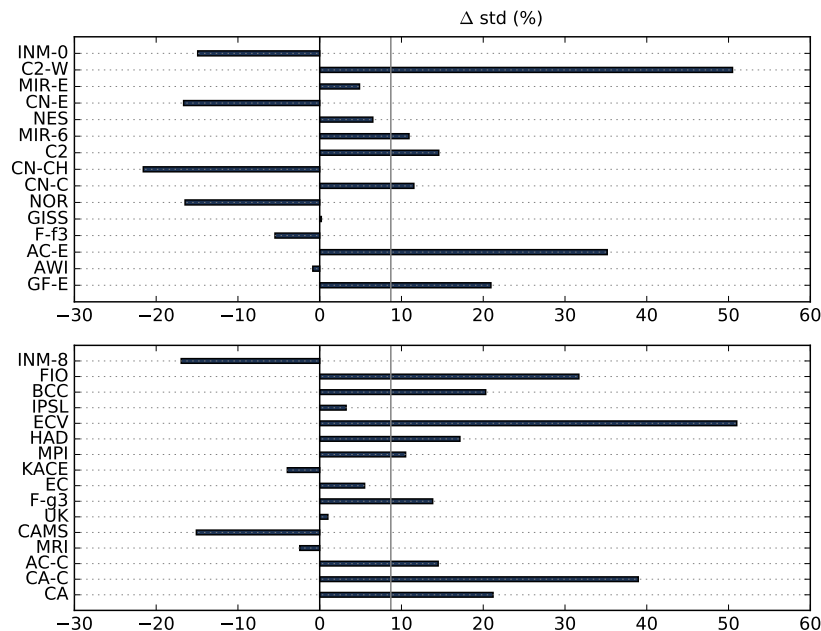
Figure F1. As in Fig. 9 but for SSP1-2.6.

References

Acharya, P. and Sreekesh, S.: Seasonal variability in aerosol optical depth over India: a spatio-temporal analysis using the MODIS aerosol product, International journal of remote sensing, 34, 4832–4849, https://doi.org/10.1080/01431161.2013.782114, 2013.

Allan, R., Barlow, M., Byrne, M. P., Cherchi, A., Douville, H., Fowler, H. J., Gan, T. Y., Pendergrass, A. G., Rosenfeld, D., Swann, A. L., Wilcox, L. J., and Zolina, O.: Advances in understanding large-scale responses of the water cycle to climate change, Annals of the New York Academy of Sciences, 1472, 1–27, https://doi.org/10.1111/nyas.14337, 2020.

Asharaf, S. and Ahrens, B.: Indian summer monsoon rainfall processes in climate change scenarios, Journal of Climate, 28, 5414–5429, https://doi.org/10.1175/JCLI-D-14-00233.1, 2015.

Ashfaq, M., Rastogi, D., Mei, R., Touma, D., and Leung, L. R.: Sources of errors in the simulation of south Asian summer monsoon in the CMIP5 GCMs, Climate Dynamics, 49, 193–223, https://doi.org/10.1007/s00382-016-3337-7, 2017.

Azad, S. and Rajeevan, M.: Possible shift in the ENSO-Indian monsoon rainfall relationship under future global warming, Scientific reports, 6, 20 145, https://doi.org/10.1038/srep20145, 2016.

Bollasina, M. A.: Hydrology: Probing the monsoon pulse, Nature Climate Change, 4, 422–423, https://doi.org/10.1038/nclimate2243, 2014.

Bollasina, M. A., Ming, Y., and Ramaswamy, V.: Anthropogenic aerosols and the weakening of the South Asian summer monsoon, Science, 334, 502–505, https://doi.org/10.1126/science.1204994, 2011.

Boos, W. R. and Korty, R. L.: Regional energy budget control of the intertropical convergence zone and application to mid-Holocene rainfall, Nature Geoscience, 9, 892–897, https://doi.org/10.1038/ngeo2833, 2016.

Byrne, M. P. and Schneider, T.: Narrowing of the ITCZ in a warming climate: Physical mechanisms, Geophysical Research Letters, 43, 11–350, 2016.

Chaturvedi, R. K., Joshi, J., Jayaraman, M., Bala, G., and Ravindranath, N.: Multi-model climate change projections for India under representative concentration pathways, Current Science, 103, 791–802, http://eprints.iisc.ac.in/45488/1/cur_sci_103-7_791_2012.pdf(lastchecked: 2021-01-20), 2012.

Cherchi, A., Alessandri, A., Masina, S., and Navarra, A.: Effects of increased CO2 levels on monsoons, Climate Dynamics, 37, 83–101, https://doi.org/10.1007/s00382-010-0801-7, 2011.

Cucchi, M., Weedon, G. P., Amici, A., Bellouin, N., Lange, S., Müller Schmied, H., Hersbach, H., and Buontempo, C.: WFDE5: bias-adjusted ERA5 reanalysis data for impact studies, Earth System Science Data, 12, 2097–2120, https://doi.org/10.5194/essd-12-2097-2020, 2020.

D'Agostino, R., Bader, J., Bordoni, S., Ferreira, D., and Jungclaus, J.: Northern Hemisphere Monsoon Response to Mid-Holocene Orbital Forcing and Greenhouse Gas-Induced Global Warming, Geophysical Research Letters, 46, 1591–1601, https://doi.org/10.1029/2018GL081589, 2019.

Dai, A., Li, H., Sun, Y., Hong, L.-C., Chou, C., and Zhou, T.: The relative roles of upper and lower tropospheric thermal contrasts and tropical influences in driving Asian summer monsoons, Journal of Geophysical Research: Atmospheres, 118, 7024–7045, https://doi.org/10.1002/jgrd.50565, 2013.

Danielsen, E. F.: In situ evidence of rapid, vertical, irreversible transport of lower tropospheric air into the lower tropical stratosphere by convective cloud turrets and by larger-scale upwelling in tropical cyclones, Journal of Geophysical Research: Atmospheres, 98, 8665–8681, https://doi.org/10.1029/92JD02954, 1993.

DeFries, R., Mondal, P., Singh, D., Agrawal, I., Fanzo, J., Remans, R., and Wood, S.: Synergies and trade-offs for sustainable agriculture: Nutritional yields and climate-resilience for cereal crops in Central India, Global Food Security, 11, 44–53, https://doi.org/10.1016/j.gfs.2016.07.001, 2016.

Deser, C., Phillips, A. S., and Alexander, M. A.: Twentieth century tropical sea surface temperature trends revisited, Geophysical Research Letters, 37, 1–6, https://doi.org/10.1029/2010GL043321, 2010.

Gadgil, S. and Gadgil, S.: The Indian monsoon, GDP and agriculture, Economic and political weekly, pp. 4887–4895, 2006.

Golyandina, N. and Zhigljavsky, A.: Singular Spectrum Analysis for time series, Springer Science & Business Media, 2013.

Gusain, A., Ghosh, S., and Karmakar, S.: Added value of CMIP6 over CMIP5 models in simulating Indian summer monsoon rainfall, Atmospheric Research, 232, 104 680, https://doi.org/10.1016/j.atmosres.2019.104680, 2020.

Herzschuh, U., Borkowski, J., Schewe, J., Mischke, S., and Tian, F.: Moisture-advection feedback supports strong early-to-mid Holocene monsoon climate on the eastern Tibetan Plateau as inferred from a pollen-based reconstruction, Palaeogeography, Palaeoclimatology, Palaeoecology, 402, 44–54, https://doi.org/10.1016/j.palaeo.2014.02.022, 2014.

Jalihal, C., Srinivasan, J., and Chakraborty, A.: Modulation of Indian monsoon by water vapor and cloud feedback over the past 22,000 years, Nature communications, 10, 1–8, https://doi.org/10.1038/s41467-019-13754-6, 2019.

Jayasankar, C., Surendran, S., and Rajendran, K.: Robust signals of future projections of Indian summer monsoon rainfall by IPCC AR5 climate models: Role of seasonal cycle and interannual variability, Geophysical Research Letters, 42, 3513–3520, https://doi.org/10.1002/2015GL063659, 2015.

Jin, Q. and Wang, C.: A revival of Indian summer monsoon rainfall since 2002, Nature Climate Change, 7, 587–594, https://doi.org/10.1038/nclimate3348, 2017.

Kim, H.: Global Soil Wetness Project Phase 3 Atmospheric Boundary Conditions (Experiment 1) [Data set]. Data Integration and Analysis System (DIAS)., https://doi.org/10.20783/DIAS.501(lastchecked:2021-01-20), 2017.

Kitoh, A.: The Asian monsoon and its future change in climate models: A review, Journal of the Meteorological Society of Japan. Ser. II, 95, 7–33, https://doi.org/10.2151/jmsj.2017-002, 2017.

Kitoh, A., Yukimoto, S., Noda, A., and Motoi, T.: Simulated changes in the Asian summer monsoon at times of increased atmospheric CO2, Journal of the Meteorological Society of Japan. Ser. II, 75, 1019–1031, https://doi.org/10.2151/jmsj1965.75.6_1019, 1997.

Knutti, R., Sedláček, J., Sanderson, B. M., Lorenz, R., Fischer, E. M., and Eyring, V.: A climate model projection weighting scheme accounting for performance and interdependence, Geophysical Research Letters, 44, 1909–1918, https://doi.org/10.1002/2016GL072012, 2017.

Krishna Moorthy, K., Suresh Babu, S., Manoj, M., and Satheesh, S.: Buildup of aerosols over the Indian Region, Geophysical Research Letters, 40, 1011–1014, https://doi.org/10.1002/grl.50165, 2013.

Kumar, K. K., Rajagopalan, B., Hoerling, M., Bates, G., and Cane, M.: Unraveling the mystery of Indian monsoon failure during El Niño, Science, 314, 115–119, https://doi.org/10.1126/science.1131152, 2006.

Lange, S.: Trend-preserving bias adjustment and statistical downscaling with ISIMIP3BASD (v1.0), Geoscientific Model Development, 12, 3055–3070, https://doi.org/10.5194/gmd-12-3055-2019, https://gmd.copernicus.org/articles/12/3055/2019/, 2019.

Lee, J.-Y. and Wang, B.: Future change of global monsoon in the CMIP5, Climate Dynamics, 42, 101–119, https://doi.org/10.1007/s00382-012-1564-0, 2014.

Levermann, A., Schewe, J., Petoukhov, V., and Held, H.: Basic mechanism for abrupt monsoon transitions, Proceedings of the National Academy of Sciences, 106, 20 572–20 577, https://doi.org/10.1073/pnas.0901414106, 2009.

Li, K., Liu, X., Wang, Y., Herzschuh, U., Ni, J., Liao, M., and Xiao, X.: Late Holocene vegetation and climate change on the southeastern Tibetan Plateau: Implications for the Indian Summer Monsoon and links to the Indian Ocean Dipole, Quaternary Science Reviews, 177, 235–245, https://doi.org/10.1016/j.quascirev.2017.10.020, 2017.

Mei, R., Ashfaq, M., Rastogi, D., Leung, L. R., and Dominguez, F.: Dominating controls for wetter South Asian summer monsoon in the twenty-first century, Journal of Climate, 28, 3400–3419, https://doi.org/10.1175/JCLI-D-14-00355.1, 2015.

Menon, A., Levermann, A., Schewe, J., Lehmann, J., and Frieler, K.: Consistent increase in Indian monsoon rainfall and its variability across CMIP-5 models, Earth System Dynamics, 4, 287–300, https://doi.org/10.5194/esd-4-287-2013, 2013.

Ming, G., Zhou, W., Cheng, P., Wang, H., Xian, F., Fu, Y., Wu, S., and Du, H.: Lacustrine record from the eastern Tibetan Plateau associated with Asian summer monsoon changes over the past 6 ka and its links with solar and ENSO activity, Climate Dynamics, 55, 1075–1086, https://doi.org/10.1007/s00382-020-05312-4, 2020.

Mishra, V., Smoliak, B. V., Lettenmaier, D. P., and Wallace, J. M.: A prominent pattern of year-to-year variability in Indian Summer Monsoon Rainfall, Proceedings of the National Academy of Sciences, 109, 7213–7217, https://doi.org/10.1073/pnas.1119150109, 2012.

Mishra, V., Kumar, D., Ganguly, A. R., Sanjay, J., Mujumdar, M., Krishnan, R., and Shah, R. D.: Reliability of regional and global climate models to simulate precipitation extremes over India, Journal of Geophysical Research: Atmospheres, 119, 9301–9323, https://doi.org/10.1002/2014JD021636, 2014a.

Mishra, V., Shah, R., and Thrasher, B.: Soil moisture droughts under the retrospective and projected climate in India, Journal of Hydrometeorology, 15, 2267–2292, https://doi.org/10.1175/JHM-D-13-0177.1, 2014b.

400 Ogata, T., Ueda, H., Inoue, T., Hayasaki, M., Yoshida, A., Watanabe, S., Kira, M., Ooshiro, M., and Kumai, A.: Projected future changes in the Asian monsoon: a comparison of CMIP3 and CMIP5 model results, Journal of the Meteorological Society of Japan. Ser. II, 92, 207–225, https://doi.org/10.2151/jmsj.2014-302, 2014.

O'Neill, B. C., Kriegler, E., Ebi, K. L., Kemp-Benedict, E., Riahi, K., Rothman, D. S., van Ruijven, B. J., Van Vuuren, D. P., Birkmann, J., Kok, K., Levy, M., and Solecki, W.: The roads ahead: Narratives for shared socioeconomic pathways describing world futures in the 21st
405 century, Global Environmental Change, 42, 169–180, https://doi.org/10.1016/j.gloenvcha.2015.01.004, 2017.

Prasanna, V.: Impact of monsoon rainfall on the total foodgrain yield over India, Journal of earth system science, 123, 1129–1145, https://doi.org/10.1007/s12040-014-0444-x, 2014.

Ramanathan, V., Chung, C., Kim, D., Bettge, T., Buja, L., Kiehl, J. T., Washington, W. M., Fu, Q., Sikka, D. R., and Wild, M.: Atmospheric brown clouds: Impacts on South Asian climate and hydrological cycle, Proceedings of the National Academy of Sciences, 102, 5326–5333,
410 https://doi.org/10.1073/pnas.0500656102, 2005.

Ramesh, K. and Goswami, P.: Assessing reliability of regional climate projections: the case of Indian monsoon, Scientific reports, 4, 1–9, https://doi.org/10.1038/srep04071, 2014.

Revadekar, J. and Preethi, B.: Statistical analysis of the relationship between summer monsoon precipitation extremes and foodgrain yield over India, International Journal of Climatology, 32, 419–429, https://doi.org/10.1002/joc.2282, 2012.

415 Roxy, M. K., Ritika, K., Terray, P., Murtugudde, R., Ashok, K., and Goswami, B.: Drying of Indian subcontinent by rapid Indian Ocean warming and a weakening land-sea thermal gradient, Nature communications, 6, 1–10, https://doi.org/10.1038/ncomms8423, 2015.

Sabeerali, C., Rao, S. A., Dhakate, A., Salunke, K., and Goswami, B.: Why ensemble mean projection of south Asian monsoon rainfall by CMIP5 models is not reliable?, Climate Dynamics, 45, 161–174, https://doi.org/10.1007/s00382-014-2269-3, 2015.

Saha, A., Ghosh, S., Sahana, A., and Rao, E.: Failure of CMIP5 climate models in simulating post-1950 decreasing trend of Indian monsoon,
420 Geophysical Research Letters, 41, 7323–7330, https://doi.org/10.1002/2014GL061573, 2014.

Schewe, J., Levermann, A., and Cheng, H.: A critical humidity threshold for monsoon transitions, Climate of the Past, 8, 535–544, https://doi.org/10.5194/cp-8-535-2012, 2012.

Schneider, U., Becker, A., Finger, P., Meyer-Christoffer, A., and Ziese, M.: GPCC Full Data Monthly Product Version 2018 at 0.5°: Monthly land-surface precipitation from rain-gauges built on GTS-based and historical data, 10.5676/DWD_GPCC/FD_M_V2018_
425 050(lastchecked:2021-01-20), 2018.

Seth, A., Rauscher, S. A., Biasutti, M., Giannini, A., Camargo, S. J., and Rojas, M.: CMIP5 projected changes in the annual cycle of precipitation in monsoon regions, Journal of climate, 26, 7328–7351, https://doi.org/10.1175/JCLI-D-12-00726.1, 2013.

Seth, A., Giannini, A., Rojas, M., Rauscher, S. A., Bordoni, S., Singh, D., and Camargo, S. J.: Monsoon responses to climate changes—connecting past, present and future, Current Climate Change Reports, 5, 63–79, https://doi.org/10.1007/s40641-019-00125-y, 2019.

430 Shah, H. L. and Mishra, V.: Hydrologic changes in Indian subcontinental river basins (1901–2012), Journal of Hydrometeorology, 17, 2667–2687, https://doi.org/10.1175/JHM-D-15-0231.1, 2016.

Sharmila, S., Joseph, S., Sahai, A. K., Abhilash, S., and Chattopadhyay, R.: Future projection of Indian summer monsoon variability under climate change scenario: An assessment from CMIP5 climate models, Global and Planetary Change, 124, 62–78, https://doi.org/10.1016/j.gloplacha.2014.11.004, 2015.

435 Shashikanth, K., Salvi, K., Ghosh, S., and Rajendran, K.: Do CMIP5 simulations of Indian summer monsoon rainfall differ from those of CMIP3?, Atmospheric Science Letters, 15, 79–85, https://doi.org/10.1002/asl2.466, 2014.

Singh, D., Ghosh, S., Roxy, M. K., and McDermid, S.: Indian summer monsoon: Extreme events, historical changes, and role of anthropogenic forcings, Wiley Interdisciplinary Reviews: Climate Change, 10, 1–35, https://doi.org/10.1002/wcc.571, 2019.

Sooraj, K., Terray, P., and Mujumdar, M.: Global warming and the weakening of the Asian summer monsoon circulation: assessments from the CMIP5 models, Climate Dynamics, 45, 233–252, https://doi.org/10.1007/s00382-014-2257-7, 2015.

Sperber, K. R., Annamalai, H., Kang, I.-S., Kitoh, A., Moise, A., Turner, A., Wang, B., and Zhou, T.: The Asian summer monsoon: an intercomparison of CMIP5 vs. CMIP3 simulations of the late 20th century, Climate dynamics, 41, 2711–2744, https://doi.org/10.1007/s00382-012-1607-6, 2013.

Tebaldi, C., Debeire, K., Eyring, V., Fischer, E., Fyfe, J., Friedlingstein, P., Knutti, R., Lowe, J., O'Neill, B., Sanderson, B., Van Vuuren, D., Riahi, K., Meinshausen, M., Nicholls, Z., Hurtt, G., Kriegler, E., Lamarque, J., Meehl, G., Moss, R., Bauer, S. E., Boucher, O., Brovkin, V., Golaz, J., Gualdi, S., Guo, H., John, J. G., Kharin, S., Koshiro, T., Ma, L., Olivié, D., Panickal, S., Qiao, F., Rosenbloom, N., Schupfner, M., Seferian, R., Song, Z., Steger, C., Sellar, A., Swart, N., Tachiiri, K., Tatebe, H., Voldoire, A., Volodin, E., Wyser, K., Xin, X., Xinyao, R., Yang, S., Yu, Y., and Ziehn, T.: Climate model projections from the Scenario Model Intercomparison Project (ScenarioMIP) of CMIP6, Earth System Dynamics Discussions, 2020, 1–50, https://doi.org/10.5194/esd-2020-68, 2020.

Turner, A. G. and Annamalai, H.: Climate change and the South Asian summer monsoon, Nature Climate Change, 2, 587–595, https://doi.org/10.1038/nclimate1495, 2012.

Turner, A. G. and Slingo, J. M.: Subseasonal extremes of precipitation and active-break cycles of the Indian summer monsoon in a climate-change scenario, Quarterly Journal of the Royal Meteorological Society: A journal of the atmospheric sciences, applied meteorology and physical oceanography, 135, 549–567, https://doi.org/10.1002/qj.401, 2009.

Ul Hasson, S., Pascale, S., Lucarini, V., and Böhner, J.: Seasonal cycle of precipitation over major river basins in South and Southeast Asia: a review of the CMIP5 climate models data for present climate and future climate projections, Atmospheric Research, 180, 42–63, https://doi.org/10.1016/j.atmosres.2016.05.008, 2016.

Van Vuuren, D. P., Kriegler, E., O'Neill, B. C., Ebi, K. L., Riahi, K., Carter, T. R., Edmonds, J., Hallegatte, S., Kram, T., Mathur, R., et al.: A new scenario framework for climate change research: scenario matrix architecture, Climatic Change, 122, 373–386, 2014.

Varghese, S. J., Surendran, S., Rajendran, K., and Kitoh, A.: Future projections of Indian Summer Monsoon under multiple RCPs using a high resolution global climate model multiforcing ensemble simulations, Climate Dynamics, 54, 1315–1328, https://doi.org/10.1007/s00382-019-05059-7, 2020.

Vecchi, G. A., Soden, B. J., Wittenberg, A. T., Held, I. M., Leetmaa, A., and Harrison, M. J.: Weakening of tropical Pacific atmospheric circulation due to anthropogenic forcing, Nature, 441, 73–76, https://doi.org/10.1038/nature04744, 2006.

Wang, P., Clemens, S., Beaufort, L., Braconnot, P., Ganssen, G., Jian, Z., Kershaw, P., and Sarnthein, M.: Evolution and variability of the Asian monsoon system: state of the art and outstanding issues, Quaternary Science Reviews, 24, 595–629, https://doi.org/10.1016/j.quascirev.2004.10.002, 2005a.

Wang, Y., Cheng, H., Edwards, R. L., He, Y., Kong, X., An, Z., Wu, J., Kelly, M. J., Dykoski, C. A., and Li, X.: The Holocene Asian monsoon: links to solar changes and North Atlantic climate, Science, 308, 854–857, https://doi.org/10.1126/science.1106296, 2005b.

Wang, Y., Cheng, H., Edwards, R. L., Kong, X., Shao, X., Chen, S., Wu, J., Jiang, X., Wang, X., and An, Z.: Millennial-and orbital-scale changes in the East Asian monsoon over the past 224,000 years, Nature, 451, 1090–1093, https://doi.org/10.1038/nature06692, 2008.

Wang, Y., Bekeschus, B., Handorf, D., Liu, X., Dallmeyer, A., and Herzschuh, U.: Coherent tropical-subtropical Holocene see-saw moisture patterns in the Eastern Hemisphere monsoon systems, Quaternary Science Reviews, 169, 231–242, https://doi.org/10.1016/j.quascirev.2017.06.006, 2017.

475 Wang, Y., Shen, J., Wang, Y., Liu, X., Cao, X., and Herzschuh, U.: Abrupt mid-Holocene decline in the Indian Summer Monsoon caused by tropical Indian Ocean cooling, Climate Dynamics, 55, 1961–1977, https://doi.org/10.1007/s00382-020-05363-7, 2020.

Wyser, K., Noije, T. v., Yang, S., Hardenberg, J. v., O'Donnell, D., and Döscher, R.: On the increased climate sensitivity in the EC-Earth model from CMIP5 to CMIP6, Geoscientific Model Development, 13, 3465–3474, https://doi.org/10.5194/gmd-13-3465-2020, 2020.

Zaveri, E., Grogan, D. S., Fisher-Vanden, K., Frolking, S., Lammers, R. B., Wrenn, D. H., Prusevich, A., and Nicholas, R. E.: Invisible water, 480 visible impact: groundwater use and Indian agriculture under climate change, Environmental Research Letters, 11, 084 005, 2016.

Zelinka, M. D., Myers, T. A., McCoy, D. T., Po-Chedley, S., Caldwell, P. M., Ceppi, P., Klein, S. A., and Taylor, K. E.: Causes of higher climate sensitivity in CMIP6 models, Geophysical Research Letters, 47, e2019GL085 782, https://doi.org/10.1029/2019GL085782, 2020.

Zhang, P., Cheng, H., Edwards, R. L., Chen, F., Wang, Y., Yang, X., Liu, J., Tan, M., Wang, X., Liu, J., An, C., Dai, Z., Zhou, J., Zhang, D., Jia, J., Jin, L., and Johnson, K. R.: A test of climate, sun, and culture relationships from an 1810-year Chinese cave record, Science, 322, 485 940–942, https://doi.org/10.1126/science.1163965, 2008.

Zhang, W., Zhang, Z., Liao, Z., Wang, Y., Chen, S., Shao, Q., and Wang, Y.: Changes in the Asian monsoon climate during the late last interglacial recorded in oxygen isotopes of a stalagmite from the Yongxing Cave, central China, Journal of Asian Earth Sciences, 179, 211–218, https://doi.org/10.1016/j.jseaes.2019.04.024, 2019.

Zhou, T., Yu, R., Li, H., and Wang, B.: Ocean forcing to changes in global monsoon precipitation over the recent half-century, Journal of 490 Climate, 21, 3833–3852, https://doi.org/10.1175/2008JCLI2067.1, 2008.